2007

Functional characterization of roles of histone deacetylases in the regulation of DNA damage response

Zhigang Yuan
University of South Florida

Functional Characterization of Roles of Histone Deacetylases in the Regulation of DNA Damage Response

by

Zhigang Yuan

A dissertation submitted in partial fulfillment
of the requirements for the degree of
Doctor of Philosophy
Department of Molecular Medicine
College of Medicine
University of South Florida

Co-Major Professor: Edward Seto, Ph.D.
Co-Major Professor: Peter Medveczky, M.D.
Jiandong Chen, Ph.D.
Burt Anderson, Ph.D.

Date of Approval:
September 13, 2007

Keywords: SIRT1, NBS1, HDAC9, ATDC, p53, protein acetylation

ACKNOWLEDGEMENTS

First of all, I would like to give thanks to my great advisor, Dr. Seto, for his research direction, his patience, and his generous financial support. I would also like to thank Dr. Xiaohong Zhang, who taught me lots of research techniques and did great collaborative work. My gratitude also extends to other members of my dissertation committee, Dr. Medveczky, Dr. Anderson, Dr. Chen and Dr. Harton. Thanks to Dr. Pross for supporting me to apply for the American Heart Association Predoctoral Fellowship. Thanks to Dr. Klein, Dr. Ugen and Dr. Solomonson for the help for my graduate study. Special thanks to Dr. Yang for taking the time to come and chair my examination committee.

I will not forget Sally Baker, Kathy Zahn, Betty Sellers, Susan Chapman, Helen Chen-Duncan, and Donna Blaha, who took care of all the administrative works and made my graduate student life much less stessful. I also would like to give thanks to my classmate and friend Joe Chou for his generous help in my graduate study and routine daily life. Thanks to the former graduate student Lily Lu for her help in my graduate study.

I appreciate the help from members of Dr. Seto's lab, past and present, the predoctoral fellowship granted from American Heart Association, the technical

support received from the Moffitt core facilities, and the help from other internal and external labs who generously provided plasmids for facilitating my research.

And, last but not least, my utmost gratitude goes to my family, my mom and dad, my mother-in-law and father-in-law, my brothers and sisters, for their love, support and taking care of my little son. Especial thanks to my wife Huayan Hou for her understanding and unwavering support.

TABLE OF CONTENTS

LIST OF FIGURES

FUNCTIONAL CHARACTERIZATION OF ROLES OF HISTONE DEACETYLASES IN THE REGULATION OF DNA DAMAGE RESPONSE

ZHIGANG YUAN

ABSTRACT

Histone deacetylases (HDACs) are a family of enzymes whose functions have been overwhelmingly associated with gene expression and chromatin dynamics by modifying the histone tails. In recent years, intensive studies have demonstrated that many non-histone proteins also could serve as substrates for HDACs. And their functions and activities have been found to be regulated by posttranslational acetylation on the ε-amino group of lysines. Here, we report that two DNA repair factors including NBS1 (Nijmegen breakage syndrome 1) and ATDC (Ataxia-Telangiectasia Group D Complementing) are acetylated proteins. SIRT1 could maintain NBS1 in a hypoacetylated state, which is required for ionizing radiation-induced NBS1 Ser343 phosphorylation. And by modulating the acetylation of ATDC, HDAC9 could prevent ATDC-p53 complex formation, promoting IR-induced cell death. These data suggest HDACs play much wider roles in cells in addition to their transcriptional repression function.

SECTION I

SIRT1 REGULATES THE FUNCTION OF THE NIJMEGEN BREAKAGE SYNDROME PROTEIN

Abstract

MRE11-RAD50-NBS1 (MRN) is a conserved nuclease complex that exhibits properties of a DNA damage sensor and is critical in regulating cellular responses to DNA double-strand breaks. NBS1, which is mutated in the human genetic disease Nijmegen breakage syndrome, serves as the regulatory subunit of MRN. Phosphorylation of NBS1 by the ATM kinase is necessary for both activation of the S-phase checkpoint and for efficient DNA damage repair response. Here, we report that NBS1 is an acetylated protein and that the acetylation level is tightly regulated by the SIRT1 deacetylase. SIRT1 associates with the MRN complex and, importantly, maintains NBS1 in a hypoacetylated state, which is required for ionizing radiation-induced NBS1 Ser343 phosphorylation. Our results demonstrate the presence of crosstalk between two different posttranslational modifications in NBS1 and strongly suggest that deacetylation of NBS1 by SIRT1 plays a key role in the dynamic regulation of the DNA damage response and in the maintenance of genomic stability.

Introduction

Nijmegen breakage syndrome (NBS) is a rare autosomal recessive condition of chromosomal instability that is clinically manifested by symptoms including microcephaly, a distinct facial appearance, growth retardation, immunodeficiency, radiation sensitivity, and a strong predisposition to lymphoid malignancy (van der Burgt et al., 1996; Shiloh, 1997; Digweed and Sperling, 2004). Cells from NBS patients exhibit radiation hypersensitivity, radioresistant DNA synthesis (RDS), chromosomal instability, and cell cycle checkpoint defect (Tauchi et al., 2002). Mutations in NBS1 (also known as nibrin or p95), the product of the Nijmegen breakage syndrome gene, are responsible for NBS (Varon et al., 1998). The N-terminus of NBS1 protein contains a forkhead-associated (FHA) domain adjacent to a breast cancer carboxy-terminal (BRCT) domain, both of which are commonly found in cell cycle checkpoint proteins. The C-terminus of NBS1 is required for induction of MRN complex-mediated apoptosis in response to irradiation (Stracker et al., 2007).

The ATM protein kinase, a multi-tasking DNA damage sensor, is mutated in individuals with the radiosensitivity disorder ataxia-telangiectasia. Following cellular exposure to ionizing radiation (IR), ATM undergoes rapid autophosphorylation at Ser1981, resulting in the conversion of the inactive dimer form to active monomers (Bakkenist and Kastan, 2003). Activated ATM phosphorylates a number of cellular substrates including NBS1 (Lim et al., 2000; Wu et al., 2000; Zhao et al., 2000). NBS1 associates with MRE11 and RAD50 to form a protein complex (MRN complex) involved in detection, signaling, and

repair of DNA damage. Using an Nbs1 knockout cell line, NBS1 was shown to be essential for homologous recombination DNA repair in vertebrate cells (Tauchi et al., 2002). Although phosphorylation of NBS1 does not affect MRN association, this modification is functionally important since mutant NBS1 (S343A) cannot completely complement radiosensitivity in cell lines lacking functional NBS1 (NBS cells) (Gatei et al., 2000; Lim et al., 2000; Zhao et al., 2000). In addition to serving as a downstream effector of ATM, NBS1 may function in activating ATM (Cerosaletti et al., 2006; Lee and Paull, 2005; You et al., 2005). In fact, NBS1 phosphorylation may be required for activation of the S-phase checkpoint by stimulating ATM-mediated phosphorylation of Chk2 (Lee and Paull, 2004).

Besides phosphorylation, the functions and activities of an increasing number of proteins have been found to be regulated by posttranslational acetylation on the ε-amino group of lysines (Glozak et al., 2005; Kouzarides, 2000; Yang, 2004). This modification prevents positive charges from forming on the amino group of lysines and, as a result, has a significant impact on the electrostatic properties of the protein. Over thirty proteins have been reported to possess lysine acetyltransferase activity, and many of these enzymes were first thought to specifically acetylate histones, but later were found to have a wide range of protein substrates in addition to histones (Sterner and Berger, 2000; Roth et al., 2001; Yang, 2004). Also, many acetyltransferases, including p300, CBP (CREB-binding protein), and PCAF (p300/CBP-associated factor) are transcriptional co-activators.

Like many covalent protein modifications, posttranslational lysine acetylation is highly reversible, and increasing evidences suggest that acetylation/deacetylation, like phosphorylation, is important in the regulation of a number of biological processes (Kouzarides, 2000). Thus, in order to fully understand the pathways that modulate the functions of NBS1, it is important to determine whether NBS1 undergoes acetylation and if so, whether this modification is reversibly regulated by deacetylation.

Histone deacetylases (HDACs) are enzymes that catalyze the removal of acetyl moieties from the ε-amino groups of conserved lysine residues in the amino terminal tail of histones. The removal of this modification strengthens histone-DNA interactions and may generate specific docking surfaces for proteins that regulate chromatin folding and/or transcription. Results from numerous studies overwhelmingly support the prediction that HDACs play crucial roles in gene transcription and most likely affect all eukaryotic biological processes that involve chromatin. Recent studies have shown that many non-histone proteins can serve as HDAC substrates and many HDACs, like histone acetyltransferases (HATs), regulate important biological processes that extend beyond histones and gene transcription (Glozak and Seto, 2005).

In humans, HDACs are divided into three categories: the class I RPD3-like proteins (HDAC1, HDAC2, HDAC3, HDAC8); the class II HDA1-like proteins (HDAC4, HDAC5, HDAC6, HDAC7, HDAC9, and HDAC10); and the class III Sir2-like proteins (SIRT1, SIRT2, SIRT3, SIRT4, SIRT5, SIRT6, and SIRT7). The class III proteins do not exhibit any sequence similarity to the other HDAC

family members and differ from the other HDACs in that they require the cofactor NAD^+ for activity. Whereas the NAD^+-dependent class III deacetylases are specifically inhibited by nicotinamide, class I and II HDACs are specifically sensitive to the inhibitor tricohostatin A (TSA).

Of the seven human Sir2-like proteins (sirtuins), SIRT1 is most similar to the yeast Sir2 protein, which is the prototypic class III HDAC (Guarente, 2006; Blander and Guarente, 2004). *In vitro*, SIRT1 preferentially deacetylates histones H4K16 and H3K9, interacts with and deacetylates histone H1 at K26, and may mediate heterochromatin formation (Vaquero et al., 2004). Besides histones, more than a dozen nonhistone proteins have been found to serve as substrates for SIRT1 (Blander and Guarente, 2004; Haigis and Guarente, 2006). SIRT1 regulates the tumor suppressor protein p53 and FOXO3 to suppress apoptosis and promote cell survival (Brunet et al., 2004; Giannakou and Partridge, 2004; Luo et al., 2001; Vaziri et al., 2001). SIRT1 plays a role in several biological processes including stress resistance, metabolism, differentiation, and aging (Haigis and Guarente, 2006). In addition, thymocytes derived from mice lacking SIRT1 exhibit increased sensitivity to -irradiation (Cheng et al., 2003).

In the present study, we show that the NBS1 protein is acetylated. Furthermore, we found that SIRT1 binds to and deacetylates NBS1 *in vitro* and *in vivo* and, importantly, maintains NBS1 in a hypoacetylated state that is required for IR-induced NBS1 phosphorylation. Induction of NBS1 hyperacetylation greatly reduces NBS1 phosphorylation. Consistent with the importance of

hypoacetylated NBS1 in DNA damage repair, cell survival decreases and RDS increases in NBS1-deficient cells complemented with hyperacetylated NBS1. Together, our findings strongly implicate crosstalk between two different posttranslational modifications in the function of NBS1. Additionally, our results uncovered NBS1 as a substrate for SIRT1 and provide convincing evidence that SIRT1 acts upstream of NBS1.

Materials and Methods

Plasmids, Antibodies, and Viruses

The following expression plasmids used in these experiments have been described previously: pcDNA3-Myc-NBS1 (Maser et al., 2001), HA-NBS1 (Lim et al., 2000), Flag-ATM (Lim et al., 2000), Flag-PCAF (Yang et al., 1996), HA-p300 (Aizawa et al., 2004), pRc/RSV-HA-CBP (Zhang et al., 2000), Flag-SIRT1-7 (Michishita et al., 2005; North et al., 2003), Myc-SIRT1 (Langley et al., 2002), GST-SIRT1 (Langley et al., 2002), and Myc-SIRT1(H363Y) (Langley et al., 2002). The plasmid encoding Myc-NBS1mt was generated using the QuickChange Site-Directed Mutagenesis kit following the manufacturer's protocol (Stratagene). Plasmids encoding GST-NBS1 deletion mutants were created by inserting PCR products of NBS1 fragments into Bam H1/Not 1 digested pGEX-5X-1 vectors (Amersham). pBS/U6-SIRT1 was constructed by inserting oligodeoxynucleotides, which targeted the sequence 5'GAAGTTGACCTCCTCATTGT3' into the pBS/U6 vector (Sui et al., 2002). SIRT1 siRNA and control siRNA adenoviruses were described previously (Rodgers et al., 2005). Plasmids that express Myc-tagged

NBS1 lysine to glutamine mutants (5KQ: K544Q/K665Q/K690Q/K698Q/K715Q; 7KQ: K441Q/K504Q/K544Q/K665Q/K690Q/K698Q/K715Q; 9KQ: K233Q/K334Q/K441Q/K504Q/K544Q/K665Q/K690Q/K698Q/K715Q; 10KQ: K208Q/K233Q/K334Q/K441Q/K504Q/K544Q/K665Q/K690Q/K698Q/K715Q) were generated by standard PCR and subcloning.

Mouse affinity purified monoclonal anti-Flag M2, rabbit affinity purified polyclonal anti-HA, and mouse monoclonal anti-acetylated-tubulin (clone 6-11B-1) antibodies were purchased from Sigma. Mouse monoclonal anti-c-Myc (clone 9E10) and mouse monoclonal anti-p53 (clone DO-1) antibodies were purchased from Santa Cruz Biotechnology. Rabbit polyclonal anti-hNBS1, rabbit polyclonal anti-phosphorylated-Ser343-hNBS1, rabbit polyclonal anti-phosphorylated-Ser343-mNbs1, and rabbit polyclonal anti-ATM were purchased from Novus Biologicals. Mouse monoclonal anti-hNBS1 (clone 34) was purchased from BD Biosciences. Protein A purified mouse monoclonal anti-phosphorylated-Ser1981-ATM (clone 10H11.E12) was purchased from Rockland Immunochemicals. Mouse monoclonal anti-hNBS1 (clone 1C3), mouse monoclonal anti-MRE11 (clone 12D7), and mouse monoclonal anti-RAD50 (clone 13B3) were purchased from GeneTex. Rabbit polyclonal anti-acetyl-lysine, rabbit polyclonal anti-SIRT1, and mouse monoclonal anti-GST (clone DG122-2A7) antibodies were purchased from Upstate (Millipore). Mouse monoclonal anti-BrdU (clone BMC9318) was purchased from Roche. Rabbit polyclonal anti-acetylated-Lys382-p53 was purchased from Cell Signaling Technology.

Cell Culture, Transfection, and Adenovirus Infection

Sirt1$^{+/-}$ mice were time-mated to screen for homozygous *Sirt1*$^{-/-}$ mutant embryos by PCR. MEFs were generated from 13.5 dpc embryos using standard methods. HeLa, 293T, and murine *Sirt1*$^{+/+}$ and *Sirt1*$^{-/-}$ fibroblasts were grown in Dulbecco's modified Eagle's medium (DMEM) supplemented with 10% fetal calf serum (FCS) and penicillin/streptomycin (pen/strep). The NBS cell line (GM07166) was obtained from Coriell Cell Repository and grown in minimum essential medium (MEM) with 10% FCS and pen/strep. All transfections were normalized with equal amounts of parental vector DNA. Transfections were performed with Lipofectamine 2000 (Invitrogen) according to the manufacturer's instructions. To generate stable cell lines, NBS cells (GM 07166) transfected with vector alone or various expression plasmids were grown in the presence of G418 (200 mg/ml, for cells that received NBS1 expression plasmids) and puromycin (0.5 mg/ml, for cells that received PCAF expression plasmids) for 10 days. Resistant colonies were isolated, pooled together, and grown for further analysis. For viral infection, HeLa cells were infected with adenovirus for 24 h in DMEM with 0.5% BSA as previously described (Rodgers et al., 2005).

Immunoprecipitation and Western Blot Analysis

For immunoprecipitations, cells were lysed in buffer (50 mM Tris-HCl [pH 7.5], 1 mM EDTA, 1% NP-40, and protease inhibitor cocktail) containing either 500 mM NaCl (high stringency) or 150 mM NaCl (low stringency). The lysates were incubated with the primary antibody overnight at 4^{o}C. The resultant

immunocomplexes were collected, washed four times in lysis buffer, and resolved by SDS-PAGE. For immunoblotting, samples were transferred onto nitrocellulose membranes. Membranes were probed with the appropriate antibodies. Proteins of interest were visualized using the Chemiluminescent Detection Kit (Pierce).

Ion Trap Mass Spectrometry

293T cells were transfected with the Myc-NBS1 expression plasmid and treated with TSA (1.3 M) and nicotinamide (20 mM) overnight. The cells were then lysed in high stringency buffer containing 10 mM NaB and 10 mM nicotinamide. Cell extracts were subjected to immunoprecipitation with anti-Myc antibodies. The immune complexes were resolved by SDS-PAGE and stained with colloidal Blue (Invitrogen). The Myc-NBS1 sequence was analyzed with an in-house algorithm (EnzOpt) for a dual enzyme strategy maximizing proteotypic peptide coverage of all lysines. The appropriate Myc-NBS1 gel band was excised and divided into two parts. Each part was subjected to in-gel reduction and carboxyamidomethylation followed by separate tryptic or chymotryptic digestion. Acetylated peptides from each digest were detected and sequenced using microcapillary reverse-phase HPLC nano-electrospray tandem mass spectrometry (LC-MS/MS) on a Thermo LTQ linear quadrupole ion trap mass spectrometer. Data analysis was facilitated with SEQUEST and the Proteomics Browser Suite (Thermo).

GST Pull-Down Assay

GST and GST-NBS1 deletion mutants were expressed and purified from bacteria using standard methods. Equimolar quantities of the various purified proteins were conjugated to glutathione-Sepharose beads and incubated with HeLa whole cell lysates for 1 h at 4°C. After extensive washing, bound proteins were eluted and analyzed by Western blotting with anti-SIRT1 antibodies.

***In Vitro* Deacetylation Assay**

In vitro deacetylation of NBS1 by SIRT1 was performed using an approach similar to that used previously for detection of PGC-1 acetylation (Nemoto et al., 2005).

RDS Assay

The RDS assay was performed as described previously (Zhao et al., 2000) with minor modifications. Briefly, NBS cells were transfected with either pEGFP-C3 (Clontech) or pEGFP-C3 and the Myc-NBS1 expression plasmid at a ratio of 1:10. In some experiments, cells were also transfected with an additional plasmid encoding Flag-PCAF. Cells were γ-irradiated with 15 Gy, incubated for 1 h at 37^{o}C, and then incubated for an additional 2 h in a medium containing 100 M of BrdU. BrdU incorporation was detected using an anti-BrdU antibody following immunostaining procedures described previously (Zhang et al., 2004).

Alternative RDS assays were performed as described by Lim et al. (2000) and by Zhao et al. (2002). Briefly, cells were labeled for 24 h in medium

containing 10 nCi/ml of ^{14}C-thymidine. The cells were washed once with PBS and then incubated for 24 h in a nonradioactive medium. After treatment with IR or left untreated, cells were incubated at 37°C for 30 min and pulse-labeled for 30 min in a medium containing 2.5 mCi/ml of ^{3}H-thymidine. Cells were then washed with PBS and lysed with 0.5 ml of 0.2 M NaOH. Radioactivity was quantified in a liquid scintillation counter, and the resulting ratios of ^{3}H/^{14}C were calculated and compared with ratios of non-irradiated cells.

Colony Survival Assay

Colony survival assays were performed as previously described (Zhao et al., 2002) with minor modifications. Briefly, NBS cells were plated in quadruplicate (1,000 cells per 60-mm tissue culture dish). The cells were γ-irradiated with 0, 2, or 5 Gy. After two weeks, dishes were washed with PBS, fixed in ice-cold methanol for 15 min, and then stained with Giemsa stain for 30 min. Colonies on each plate were quantified and expressed as the percentage of the unirradiated control.

Results

NBS1 is an Acetylated Protein

The NBS1 protein (accession BAA28616) contains three lysine acetylation consensus motifs, $Kx_{1-2}x/KK$ (Yang, 2004), at residues 233-237 (KGHKK), 683-687 (KNFKK), and 686-690 (KKFKK). Thus, in addition to phosphorylation, NBS1 is potentially modified by posttranslational lysine acetylation. To determine if NBS1 is indeed a substrate for acetyltransferases, 293T cells were co-

transfected with plasmids expressing a Myc-tagged NBS1 protein and three different acetyltransferases (PCAF, p300, or CBP). Acetylated NBS1 was readily detected in cells that overexpressed PCAF or p300 but not in cells that overexpressed CBP (Figure 1A). The level of NBS1 acetylation by PCAF was dose-dependent (Figure 1B). Analysis of purified Myc-NBS1 by LC tandem mass spectrometry (LC-MS/MS) revealed that 10 of the 70 lysine residues were acetylated. These included K208, K233, K334, K441, K504, K544, K665, K690, K698, and K715 (Figure 1C). Mutation of all ten sites from lysine to arginine resulted in a dramatic decrease in the overall NBS1 acetylation levels as determined by Western blot analysis with anti-acetyl-lysine antibodies (Figure 1D). A small amount of residual acetylation can still be detected by Western blotting with anti-acetyl-lysine antibodies, suggesting that there could be minor acetylation sites that escaped mass spectrometry analysis.

Class III HDACs Regulate NBS1 Acetylation Level

To examine whether NBS1 might be regulated by deacetylation, we immunoprecipitated Myc-NBS1 from 293T cells treated with HDAC inhibitors. As shown in Figure 1E, treatment of cells with TSA, a class I and II HDAC inhibitor, did not affect the acetylation status of NBS1. In contrast, cells treated with nicotinamide, a class III (Sir2 family) HDAC inhibitor, resulted in a notable increase in acetylation of NBS1. Treatment with a combination of TSA and nicotinamide was not associated with any additional increase in NBS1 acetylation

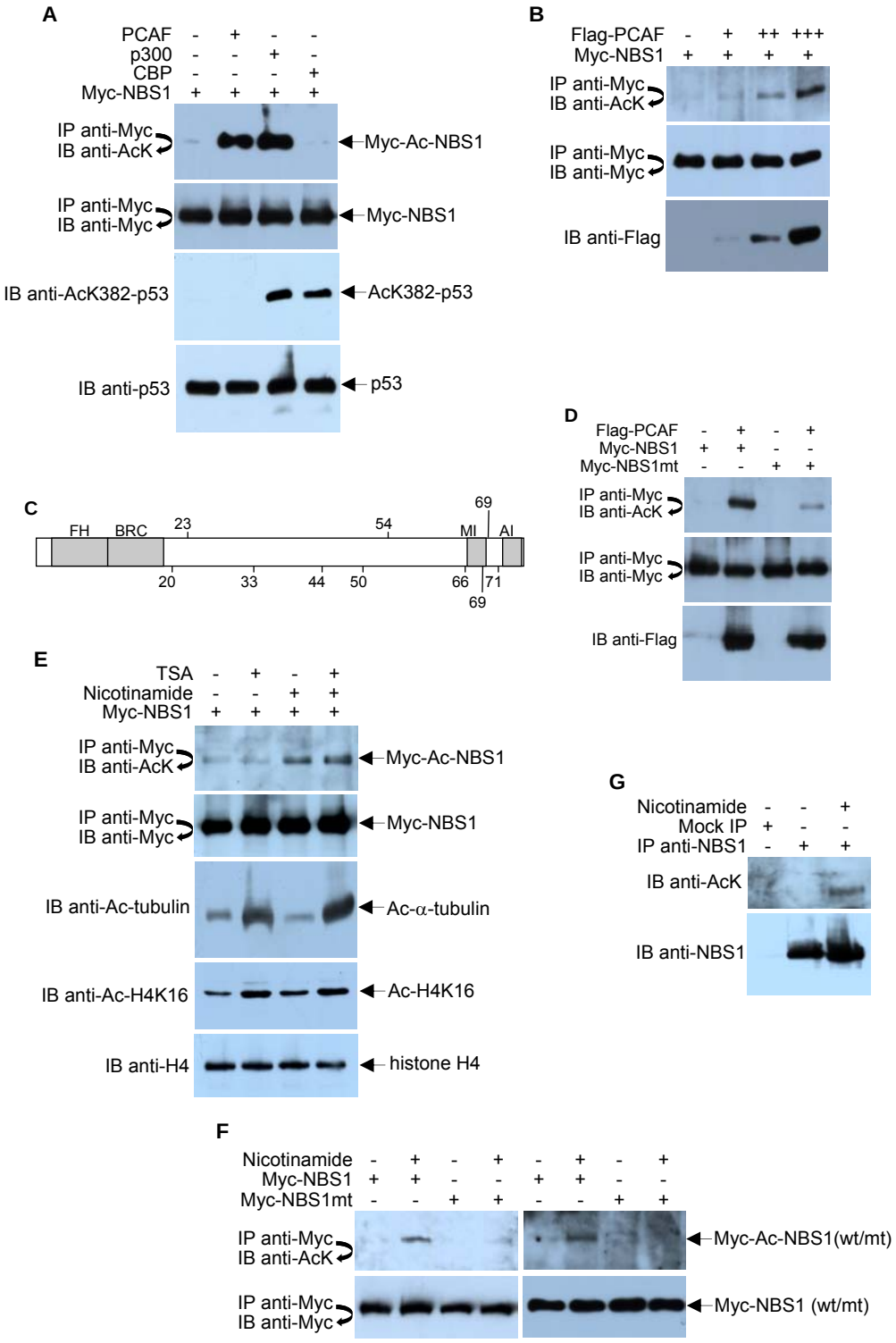

Figure 1. NBS1 is Acetylated

(A) 293T cells were co-transfected with equal amounts (4ug) of Myc-NBS1 ± one of the following expression plasmids: Flag-PCAF, HA-p300, or HA-CBP. Cell lysates were immunoprecipitated (IP) under high stringency conditions using anti-

Myc antibodies. Immunoprecipitates were subjected to Western blot (IB) analysis using anti-acetyl-lysine (AcK) antibodies. The blot was stripped and re-probed with anti-Myc antibodies to confirm equal immunoprecipitation efficiency and loading. As CBP (but not PCAF) is known to acetylate p53-K382, a Western blot was performed with anti-AcK382-p53 to confirm that the expressed CBP was functional. (B) 293T cells were co-transfected with Myc-NBS1 (4 ug) and Flag-PCAF (0, 0.5, 1, or 4 ug). Cell lysates were subjected to immunoprecipitation/Western blot analysis using the indicated antibodies. Western blot analysis of whole extracts was performed to assess PCAF expression (bottom panel). (C) Myc-NBS1, which was expressed and purified from 293T cells, was digested with trypsin and subjected to ITMS. Positions of the unambiguously-identified acetylated lysine residues are shown. FHA, forkhead-associated domain; BRCT, BRCA1 C-terminal domain; MIR, MRE11-interacting domain; AIR, ATM-interacting domain. (D) 293T cells were co-transfected with Myc-NBS1 (wild-type or lysine to arginine mutant [mt]) and Flag-PCAF (4 ug each), as indicated. Total and acetylated NBS1 levels were analyzed by immunoprecipitation/Western blotting. (E) 293T cells were transfected with plasmids that expressed Myc-NBS1 (4 ug). Twenty-four hours post-transfection, cells were left untreated or treated overnight with TSA (1.3 uM), nicotinamide (20 mM), or TSA plus nicotinamide. Cell lysates were subjected to immunoprecipitation/Western blotting. Whole cell extracts were probed with anti-Ac-tubulin and anti-Ac-H4K16 to confirm that TSA is functional under the treatment condition (lower panels). (F) 293T cells were transfected with plasmids (4 ug each) expressing wild-type or mutant Myc-NBS1 as indicated and then treated with 20 mM nicotinamide overnight. Myc-NBS1 acetylation and protein expression were examined by immunoprecipitation/Western blotting. (G) HeLa cells were treated with nicotinamide (20 mM) or left untreated overnight. Cell lysates were then immunoprecipitated under high stringency conditions with monoclonal anti-NBS1 antibodies. Endogenous acetylated NBS1 was analyzed by Western blotting with a mixture of polyclonal anti-acetyl-lysine antibodies.

when compared to treatment with nicotinamide alone. Thus, NBS1 might be deacetylated by class III HDACs but not by class I or II HDACs. Hyperacetylation of NBS1 is specific to nicotinamide treatment since the NBS1-acetylation mutant did not respond to this HDAC inhibitor (Figure 1F). Anti-acetyl-lysine Western blot analysis of anti-NBS1 immunoprecipitates obtained under high stringency conditions in which neither MRE11 nor RAD50 co-precipitated with NBS1, revealed that nicotinamide enhanced the acetylation state of endogenous NBS1 (Figure 1G), providing proof that endogenous NBS1 is regulated by class III HDACs.

NBS1 Interacts with SIRT1

An interesting feature of the class III HDACs is their subcellular location (Michishita et al., 2005). SIRT1, SIRT6, and SIRT7 are present in the nucleus while SIRT2 is located in the cytosol despite the possibility of deacetylating H4K16 during mitosis (Vaquero et al., 2006). SIRT3, SIRT4, and SIRT5 are localized in the mitochondria. Of the three nuclear SIRTs, SIRT1 has been shown to possess robust deacetylase enzymatic activity, while SIRT6 and SIRT7 have been reported to have very weak or no deacetylase activity (Liszt et al., 2005; North et al., 2003). Therefore, SIRT1 is likely responsible for the deacetylation of NBS1.

Since most, if not all, deacetylase substrates interact with their respective enzymes, we first tested the ability of NBS1 to interact with SIRT1. As shown in figure 2A, Flag-SIRT1 co-precipitated with Myc-NBS1. Similarly, Myc-NBS1 co-precipitated with Flag-SIRT1 (Figure 2B). The SIRT1-NBS1 interaction is highly specific since none of the other Sir2 family members (SIRT2, SIRT3, SIRT4, SIRT5, SIRT6, or SIRT7) co-precipitated with NBS1 under identical conditions (Figure 2C). This association of SIRT1 and NBS1 also occurs in the absence of overexpression, epitope tagging of either protein, or IR treatment (Figure 2D). Because the subunits of the MRN complex most likely do not act individually, MRE11 and RAD50 also co-precipitated with SIRT1 as expected, suggesting that SIRT1 associates with the whole MRN complex. Analyses of three different GST-NBS1 deletions indicated that SIRT1 interacts with the C-terminus of NBS1

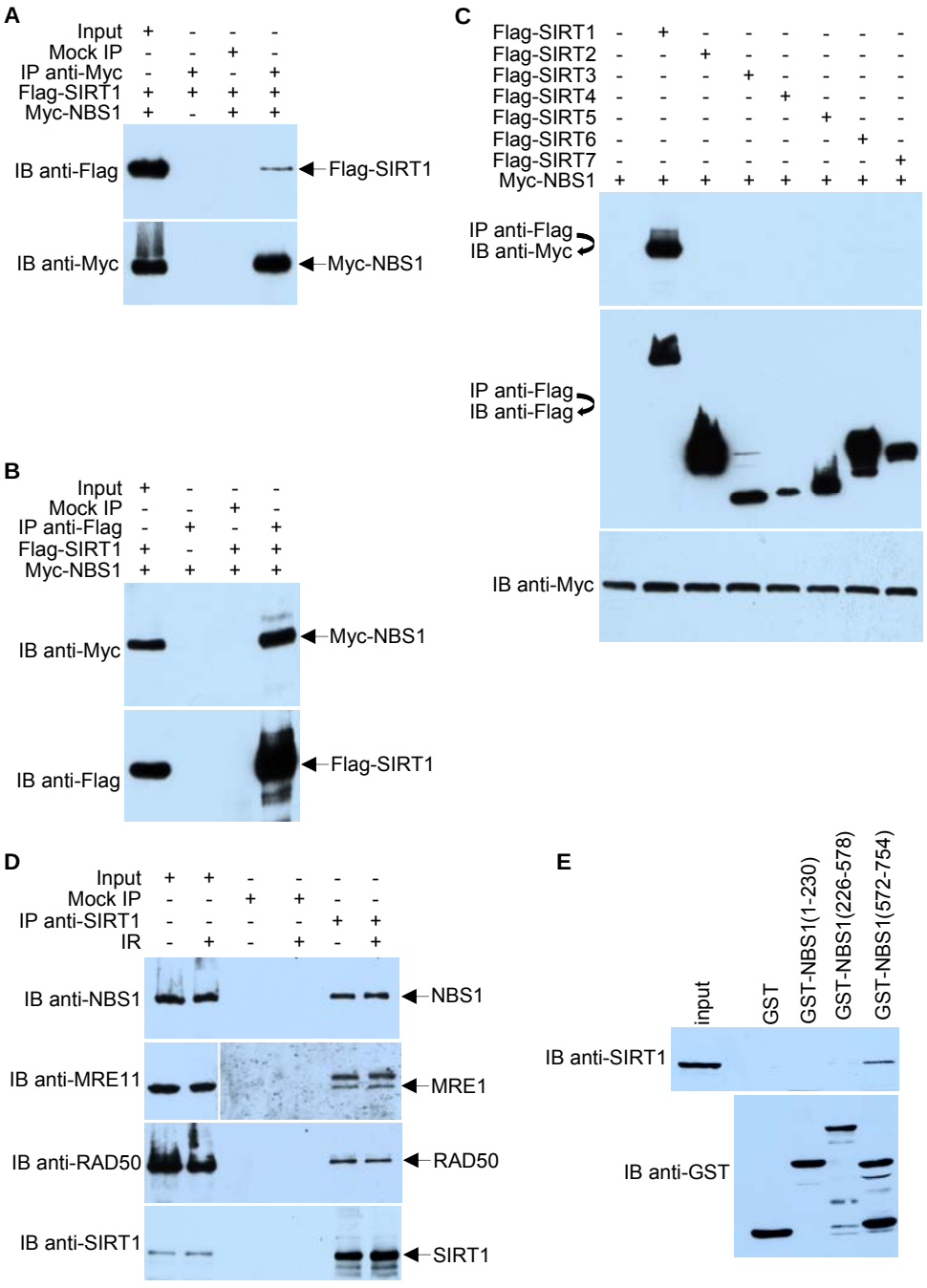

Figure 2. SIRT1 Interacts With NBS1

(A, B, C) 293T cells were co-transfected with plasmids (4ug each) encoding the indicated Myc and Flag fusion proteins. Anti-Myc and anti-Flag immunoprecipitates obtained under low stringency conditions were analyzed by Western blotting with the indicated antibodies. (D) HeLa cells were irradiated (10 Gy) or left untreated. One hour after irradiation, endogenous SIRT1 was immunoprecipitated under low stringency conditions with anti-SIRT1 polyclonal antibodies.

Immune complexes were analyzed by Western blotting with anti-NBS1, anti-MRE11, anti-RAD50, or anti-SIRT1 antibodies. For maximum clarity, the image gathered for the left upper middle panel (MRE11, lanes 1 and 2) was under-exposed compared to the right upper middle panel (MRE11, lanes 3-6). (E) GST-NBS1 deletion mutants coupled to Sepharose beads were incubated with whole HeLa cell extracts. After the beads were washed, bound proteins were eluted and analyzed by Western blotting with an anti-SIRT1 antibody. The blot was stripped and re-probed with anti-GST antibodies to confirm equal quantities of GST proteins in each reaction.

(residues 572-754), a segment that contains the MRE11 and ATM interaction region (Figure 2E).

SIRT1 Deacetylates NBS1

To test whether SIRT1 deacetylates NBS1, we examined the effect of RNAi-mediated SIRT1 knockdown on NBS1 acetylation in 293T cells. BS/U6-templated siRNA efficiently silenced expression of SIRT1 but not the control protein β-actin, as monitored by Western blot analysis (Figure 3A). In agreement with the finding that SIRT1 binds NBS1, acetylation of both Myc-NBS1 (Figure 3A) and endogenous NBS1 (Figure 3B) was significantly increased as a result of SIRT1 knockdown. Unlike knock-down of SIRT1, depletion of SIRT6 or SIRT7 did not affect NBS1 acetylation levels (Figure 3C). Furthermore, PCAF-acetylated NBS1 was deacetylated by wild-type SIRT1 (Figure 3D), but not by a catalytic-defective SIRT1 mutant (H363Y) (Figure 3D) or by SIRT2, SIRT3, SIRT4, SIRT6, SIRT7 (Figure 3E). *In vitro* deacetylation assays using purified SIRT1 in the presence of NAD^+ further confirmed that NBS1 is a substrate of SIRT1 (Figure 3F). Collectively, our data strongly suggest that SIRT1 modulates the acetylation status of NBS1 via its deacetylase activity.

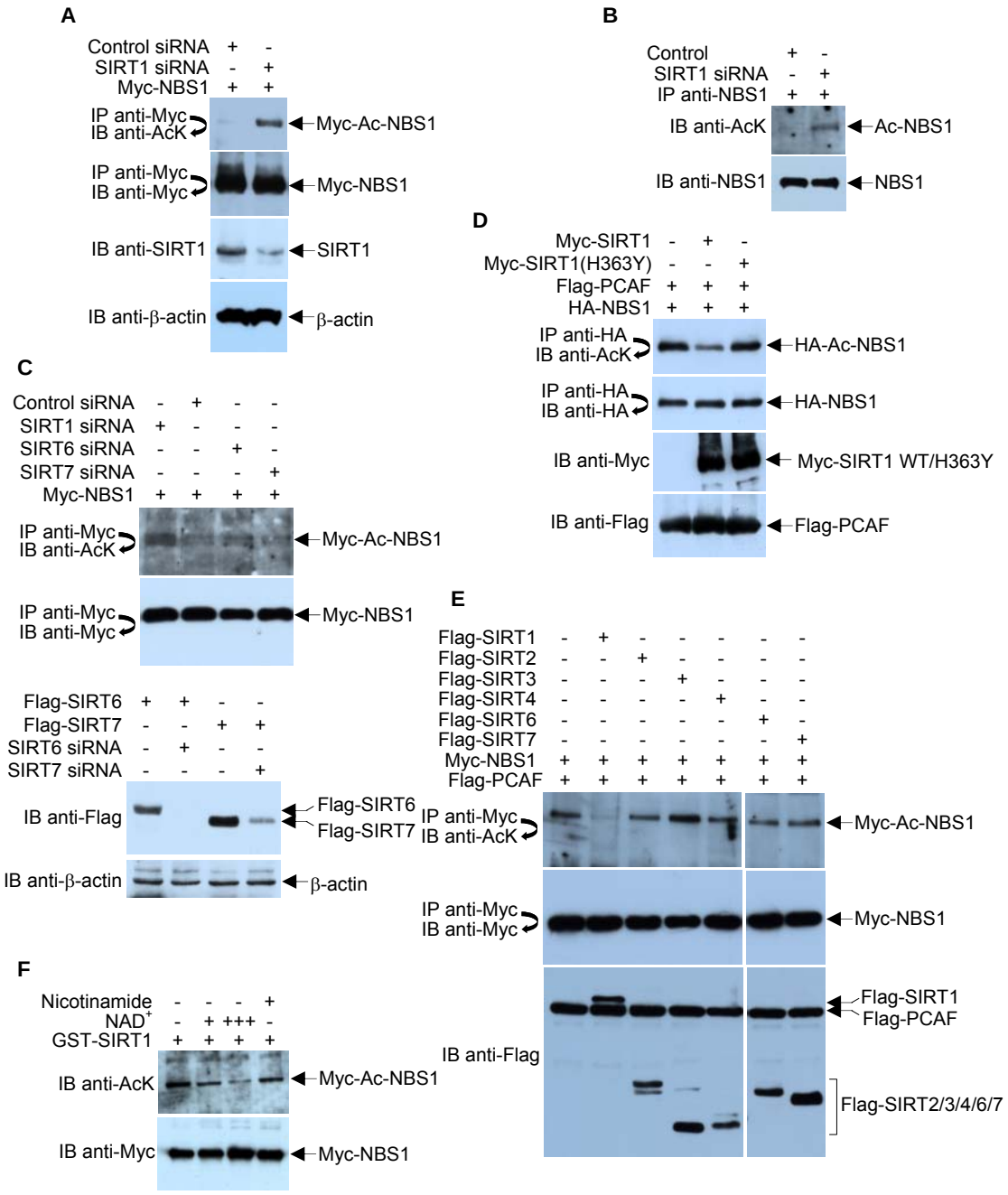

Figure 3. SIRT1 Deacetylates NBS1

(A) 293T cells were co-transfected with equal amounts (4 ug) of Myc-NBS1 plasmid and either a plasmid encoding pBS/U6-SIRT1 or control siRNA. Western blots were performed with the indicated antibodies to assess the levels of SIRT1, β-actin, total Myc-NBS1, and acetylated Myc-NBS1. (B) 293T cells were infected with either adenovirus that

expresses control siRNA or adenovirus that expresses SIRT1 siRNA. Western blots were performed with the indicated antibodies to assess the acetylation of endogenous NBS1 and NBS1 immunoprecipitation efficiency. (C) Top two panels, 293T cells were co-transfected with equal amounts (4 ug) of Myc-NBS1 plasmid and either a plasmid encoding SIRT1 siRNA, SIRT6 siRNA, SIRT7 siRNA, or control siRNA. Western blots were performed with the indicated antibodies to assess the levels of total Myc-NBS1 and acetylated Myc-NBS1. Bottom two panels, similar experiments were performed with over-expression of Flag-SIRT6 and Flag-SIRT7 to show that SIRT6 and SIRT7 siRNAs are functional. (D) 293T cells were co-transfected with plasmids that express HA-NBS1, Flag-PCAF, and either a wild-type or a catalytically-defective Myc-SIRT1. Acetylation of HA-NBS1 and all protein levels were determined with direct Western blotting or immunoprecipitations followed by Western blotting using the indicated antibodies. (E) 293T cells were co-transfected with plasmids that express Myc-NBS1, Flag-PCAF, and different Flag-tagged SIRTs. Acetylation of Myc-NBS1 and all protein levels were determined with direct Western blotting or immunoprecipitations followed by Western blotting using the indicated antibodies. (F) 293T cells were transfected with Myc-NBS1 and Flag-PCAF. Anti-Myc immunoprecipitates were incubated with recombinant GST-SIRT1 in the absence or presence of NAD^+ (lane 2, 1mM; lane 3, 10 mM) and nicotinamide (10 mM) at 30^oC for 1 h. Western blot analysis of acetylated Myc-NBS1 was then performed using anti-acetyl-lysine (AcK) antibodies.

Acetylation Inhibits NBS1 Phosphorylation

The balance between acetylation and deacetylation may have functional consequences for NBS1. Previous work has shown that ATM-mediated phosphorylation of NBS1 at Ser343 in response to DNA damage is critical for the DNA damage responses and for activation of the cell cycle S-phase checkpoint (Lim et al., 2000; Wu et al., 2000; Zhao et al., 2000). We hypothesized that different posttranslational modifications of NBS1 affect the phosphorylation of NBS1 at Ser343. NBS cells (GM07166) expressing Myc-NBS1 alone or in combination with Flag-PCAF were irradiated, and the time course of NBS1 Ser343 phosphorylation was examined via Western blot analysis. As shown in Figure 4A, overexpression of PCAF, which acetylates NBS1, reduced the levels of NBS1 phosphorylation at all times examined. Similar results were obtained

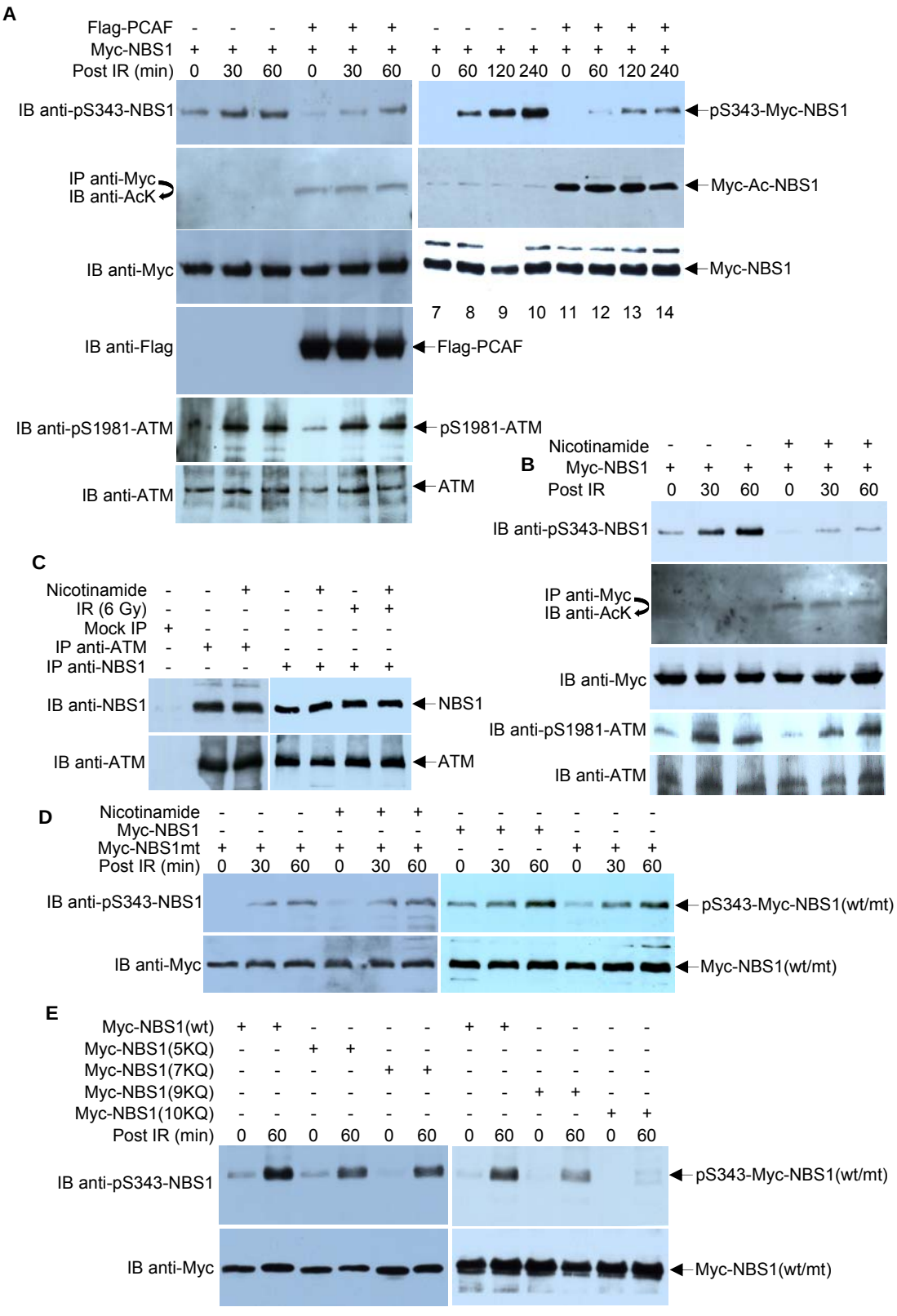
A
Flag-PCAF
Myc-NBS1
Post IR (min)
IB anti-pS343-NBS1
pS343-Myc-NBS1
IP anti-Myc
IB anti-AcK
Myc-Ac-NBS1
IB anti-Myc
Myc-NBS1
7 8 9 10 11 12 13 14
IB anti-Flag
Flag-PCAF
IB anti-pS1981-ATM
pS1981-ATM
IB anti-ATM
ATM
B
Nicotinamide
Myc-NBS1
Post IR
IB anti-pS343-NBS1
IP anti-Myc
IB anti-AcK
IB anti-Myc
IB anti-pS1981-ATM
IB anti-ATM
C
Nicotinamide
IR (6 Gy)
Mock IP
IP anti-ATM
IP anti-NBS1
IB anti-NBS1
NBS1
IB anti-ATM
ATM
D
Nicotinamide
Myc-NBS1
Myc-NBS1mt
Post IR (min)
IB anti-pS343-NBS1
pS343-Myc-NBS1(wt/mt)
IB anti-Myc
Myc-NBS1(wt/mt)
E
Myc-NBS1(wt)
Myc-NBS1(5KQ)
Myc-NBS1(7KQ)
Myc-NBS1(9KQ)
Myc-NBS1(10KQ)
Post IR (min)
IB anti-pS343-NBS1
pS343-Myc-NBS1(wt/mt)
IB anti-Myc
Myc-NBS1(wt/mt)

Figure 4. NBS1 Acetylation Status Affects IR-induced NBS1 Phosphorylation

(A) The NBS cell line GM07166 was transfected with equal amounts (4 ug) of Myc-NBS1 expression plasmid and Flag-PCAF expression plasmid or empty vector. Twenty-four hours post-transfection, cells were irradiated (6 Gy) or left untreated. Cell lysates were subjected to Western blot analysis or to high stringency immunoprecipitation/Western blot analysis, as indicated. (B) NBS cells transfected with Myc-NBS1 expression plasmid (4 ug) were treated overnight with 20 mM of nicotinamide or left untreated. The cells were then irradiated (6 Gy) or left untreated. Cell lysates were prepared after the indicated time and subjected to direct Western blot analysis or high stringency immunoprecipitation/Western blot analysis using the indicated antibodies. (C) To examine the effect of nicotinamide on ATM-NBS1 interactions, ATM and NBS1 were immunoprecipitated with anti-ATM antibodies and anti-NBS1 antibodies, respectively, from extracts prepared from HeLa cells treated ± nicotinamide. NBS1 and ATM were identified in the immunoprecipitates by Western blotting with anti-NBS1 and anti-ATM, respectively. (D) NBS cells were transfected with plasmids encoding either wild-type or acetylation-defective Myc-NBS1 (4 ug). Parallel cultures were then irradiated or left unirradiated in the presence or absence of nicotinamide. Lysates were analyzed by Western blots with the indicated antibodies. (E) NBS cells were transfected with plasmids encoding either wild-type Myc-NBS1 or acetylation-mimic Myc-NBS1 mutants (4 ug). Parallel cultures were then irradiated or left unirradiated and lysates were analyzed by Western blots with the indicated antibodies.

when NBS cells, complemented with Myc-NBS1, were treated with nicotinamide to induce NBS1 hyperacetylation (Figure 4B). The decrease in NBS1 Ser343 phosphorylation was not due to a decrease in ATM protein levels (Figures 4A and 4B), a decrease in activated ATM (as measured by phospho-S1981 of ATM; Figures 4A and 4B), or a decrease in ATM-NBS1 interaction (Figure 4C). Treatment with nicotinamide had no effect on NBS1 Ser343 phosphorylation in an NBS1 mutant that was refractory to acetylation/deacetylation (Figure 4D).

To further examine the effect of acetylation/deacetylation on NBS1 Ser343 phosphorylation, we constructed four plasmids that express NBS1 acetylation-mimic mutants, with lysine to glutamine changes, and introduced them into NBS cells. As shown in Figure 4E, consistent with our observation that acetylation of

NBS1 inhibits phosphorylation of NBS1, mutation of lysine to glutamine in NBS1 resulted in a significant decrease in NBS1 Ser343 phosphorylation. Importantly, the decrease in NBS1 phosphorylation is strictly proportional to the number of lysine mutations (i.e., the more lysine to glutamine change, the more decrease in NBS1 phosphorylation).

Presence of SIRT1 Affects NBS1 phosphorylation

Because SIRT1 is the chief regulator of the acetylation status of NBS1 (Figure 3), we determined whether NBS1 Ser343 phosphorylation was directly affected by the presence of SIRT1. As shown in Figure 5A, Nbs1 Ser343 was hypophosphorylated in *Sirt1*$^{-/-}$ MEFs compared to wild-type MEFs. Likewise, depletion of SIRT1 by siRNA resulted in a significant decrease in NBS1 Ser343 phosphorylation (Figure 5B).

Acetylation of NBS1 Affects RDS

Although results from one study suggest that ATM phosphorylation of NBS1 contributes to the formation of IR-induced foci in cells (Zhao et al., 2000), other studies convincingly demonstrated that NBS1 phosphorylation does not affect formation of IR-induced foci and that the MRN complex is recruited to foci independently of ATM (Lim et al., 2000). We examined the ability of the NBS1 acetylation-defective mutant to associate with MRE11 and RAD50 and found that no significant differences exist between mutant and wild-type NBS1 (Figure S1). Furthermore, no significant differences in NBS1 foci formation could be detected

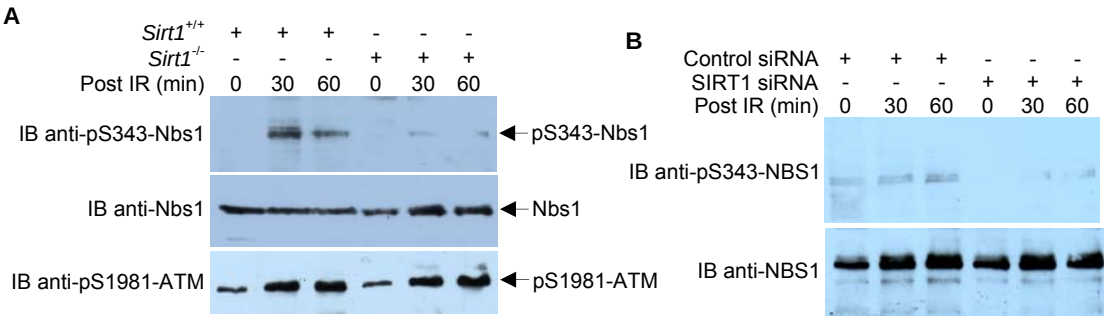

Figure 5. Presence of SIRT1 affects NBS1 Ser343 phosphorylation

(A) Murine *Sirt1*$^{+/+}$ and *Sirt1*$^{-/-}$ fibroblasts were irradiated (6 Gy) or left unirradiated. At different time points after IR, cell lysates were collected and analyzed by Western blotting with anti-pS343-mNbs1 antibodies. The blot was sequentially stripped and re-probed with anti-mNbs1 and pS1981-ATM antibodies to confirm equal mNbs1 protein levels and intact ATM activation. (B) 293T cells infected with adenoviruses expressing SIRT1 siRNA or control viruses were irradiated (6 Gy) or left unirradiated. At different time points after IR, cell lysates were collected and analyzed by Western blotting with anti-pS343-NBS1 antibodies. The blot was stripped and re-probed with anti-NBS1.

between *Sirt1*$^{+/+}$ and *Sirt1*$^{-/-}$ MEFs following IR treatment (data not shown). Therefore, our data suggest that, similar to phosphorylation, acetylation of NBS1 does not play a role in the recruitment of MRN to H2AX domains surrounding DNA DSBs.

Unlike IR-induced foci formation, phosphorylation of NBS1 is clearly involved in regulating the intra-S-phase checkpoint (Lim et al., 2000; Zhao et al., 2000). A common phenotype of NBS cells is the loss of the IR-induced S-phase checkpoint, leading to RDS. Using an RDS assay, we examined the effects of NBS1 acetylation on cell cycle checkpoints activated by DNA damage. NBS cells expressing Myc-NBS1 and enhanced green fluorescent protein (EGFP) were irradiated or mock-treated immediately after 25-bromodeoxyuridine (BrdU) treatment, and the ratios of BrdU-positive/EGFP-positive cells to EGFP-positive

cells were determined. Compared to wild-type NBS1, PCAF-hyperacetylated NBS1 was ineffective at inhibiting RDS, suggesting that hypoacetylation of NBS1 is crucial for intra-S-phase checkpoint activation (Figure 6A). In contrast, PCAF did not alter the ability of the acetylation-refractory mutant NBS1 to inhibit RDS. Similarly, in control experiments, PCAF had no effect on the NBS1 phosphorylation mutant (S343A) in inhibiting RDS. Western blot analysis confirmed that Ser343 phosphorylation of wildtype (Myc-NBS1), but not the acetylation mutant (Myc-NBS1mt), decreased with increased acetylation in NBS cells.

To be certain that NBS1 acetylation/deacetylation affects RDS, we transfected NBS cells (GM07166) with plasmids expressing wild-type or mutated NBS1, in the presence or absence of plasmids that express PCAF. Stable clones were selected by growth in G418 plus or minus puromycin, and cells stably expressing NBS1 and/or PCAF were treated with IR and examined for DNA synthesis using radiolabeled thymidine. Consistent with transient transfection results, acetylation of wild-type, but not acetylation-defective, NBS1 by PCAF significantly reduced its ability to inhibit RDS (Figure 6B).

Finally, consistent with observations that NBS1 hyperacetylation prevents its ability to inhibit RDS in transfected NBS cells, we found that *Sirt1*-/- MEFs, which contain hypophosphorylated and hyperacetylated Nbs1, display a higher level of RDS compared to *Sirt1*+/+ cells (Figure 6C).

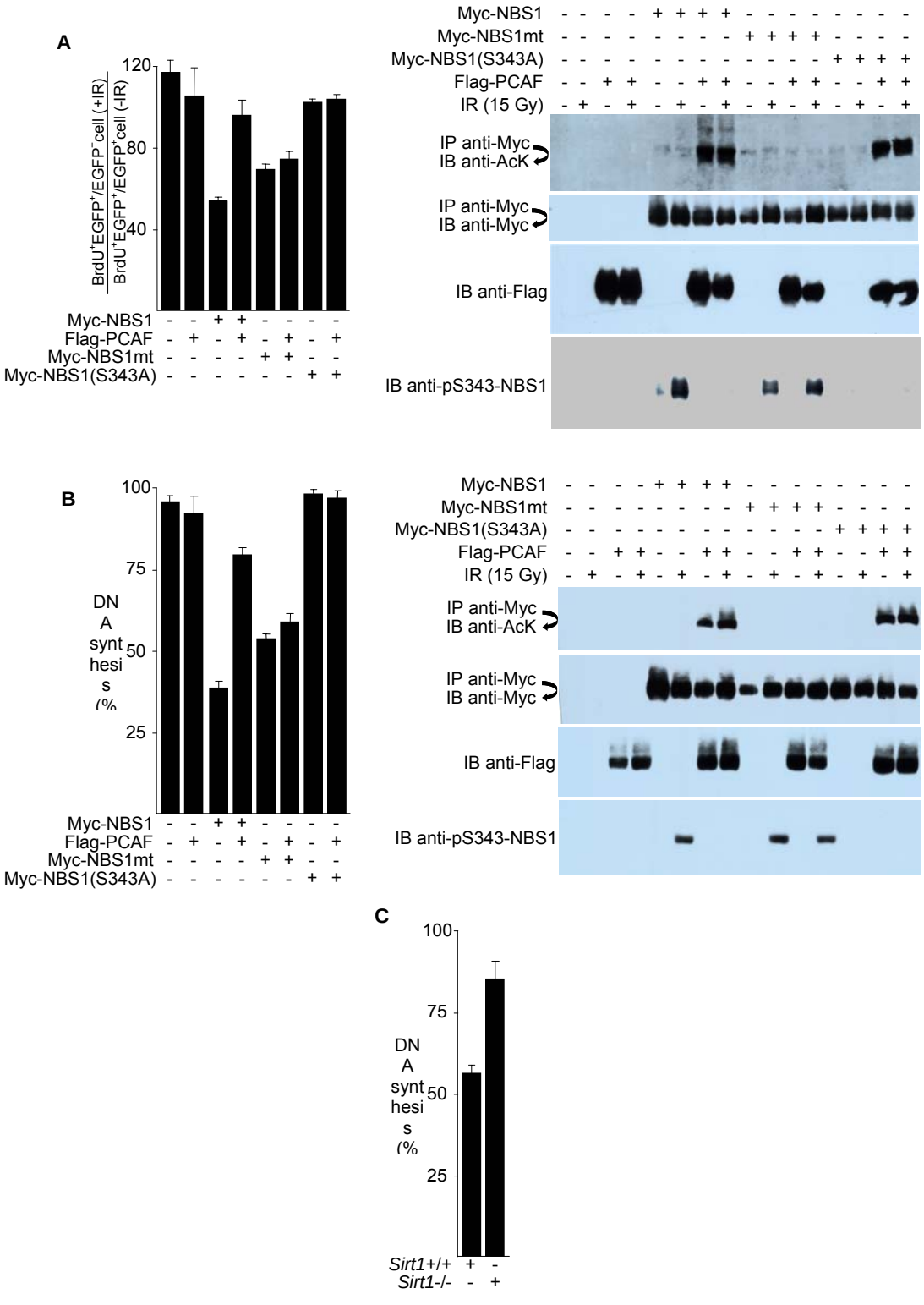
A
120
80
40
BrdU+EGFP+/EGFP+cell (+IR)
BrdU+EGFP+/EGFP+cell (-IR)
Myc-NBS1 - - + + - - - -
Flag-PCAF - + - + - + - +
Myc-NBS1mt - - - - + + - -
Myc-NBS1(S343A) - - - - - - + +
Myc-NBS1 - - - - + + + + - - - - - - - -
Myc-NBS1mt - - - - - - - - + + + + - - - -
Myc-NBS1(S343A) - - - - - - - - - - - - + + + +
Flag-PCAF - - + + - - + + - - + + - - + +
IR (15 Gy) - + - + - + - + - + - + - + - +
IP anti-Myc
IB anti-AcK
IP anti-Myc
IB anti-Myc
IB anti-Flag
IB anti-pS343-NBS1
B
100
75
50
25
DN
A
synt
hesi
s
(%
Myc-NBS1 - - + + - - - -
Flag-PCAF - + - + - + - +
Myc-NBS1mt - - - - + + - -
Myc-NBS1(S343A) - - - - - - + +
Myc-NBS1 - - - - + + + + - - - - - - - -
Myc-NBS1mt - - - - - - - - + + + + - - - -
Myc-NBS1(S343A) - - - - - - - - - - - - + + + +
Flag-PCAF - - + + - - + + - - + + - - + +
IR (15 Gy) - + - + - + - + - + - + - + - +
IP anti-Myc
IB anti-AcK
IP anti-Myc
IB anti-Myc
IB anti-Flag
IB anti-pS343-NBS1
C
100
75
50
25
DN
A
synt
hesi
s
(%
Sirt1+/+ + -
Sirt1-/- - +

Figure 6. NBS1 Acetylation Affects Radioresistant DNA synthesis (RDS)

(A) NBS cells were transfected with plasmids encoding the indicated proteins. Twenty-four hours after transfection, cells were irradiated (15 Gy) or left unirradiated. Left panel, RDS was determined by comparing the ratio of $BrdU^+/EGFP^+$ cells to $EGFP^+$ cells. The bar represents the ratio in the IR-treated cells divided by the ratio in the untreated cells. Right panels, to assess immunoprecipitation efficiency, protein expression, and NBS1 acetylation/phosphorylation, cell lysates were subjected to Western blot analysis or to high stringency immunoprecipitation/Western blot analysis, as indicated. Representative blots are shown. (B) Left panel, NBS cells (GM 07166) transfected with vector alone or the indicated expression plasmids were grown in the presence of G418 (200 mg/ml, for cells that received NBS1 expression plasmids) and puromycin (0.5 mg/ml, for cells that received PCAF expression plasmids) for 10 days. Stable colonies were isolated, pooled together, and after treatment with 15 Gy of IR or left untreated, cells were radiolabeled with thymidine for RDS analysis. Right panels, representative blots to monitor immunoprecipitation efficiency, protein expression, and NBS1 acetylation/phosphorylation. (C) 2 X 10^4 *Sirt1*+/+ or *Sirt1*-/- MEFs were plated on 35 mm dishes for 48 h. RDS assays were performed using the radio-labeling method to determine inhibition of DNA synthesis after 15 Gy of IR.

Acetylation of NBS1 Affects Cell Survival

Unsuccessful DNA damage responses are reflected in an overall decrease in cell survival. Therefore, clonogenic cell survival assays were employed to examine the importance of NBS1 acetylation in DNA damage responses. NBS cells were exposed to a sublethal dose of IR, and colonies were counted two weeks later. Cell transfection and immunoprecipitation efficiency, protein expression levels, and NBS1/NBS1mt acetylation levels were monitored by immunoprecipitation followed with Western blots or by direct Western blots (Figure 7A). Consistent with the finding that hyperacetylated NBS1 negatively affects cell cycle checkpoint activation, PCAF-hyperacetylated NBS1 was much less effective in reducing the IR sensitivity of NBS cells (increasing cell survival) than non-hyperacetylated NBS1. As expected, in the presence of PCAF, survival among

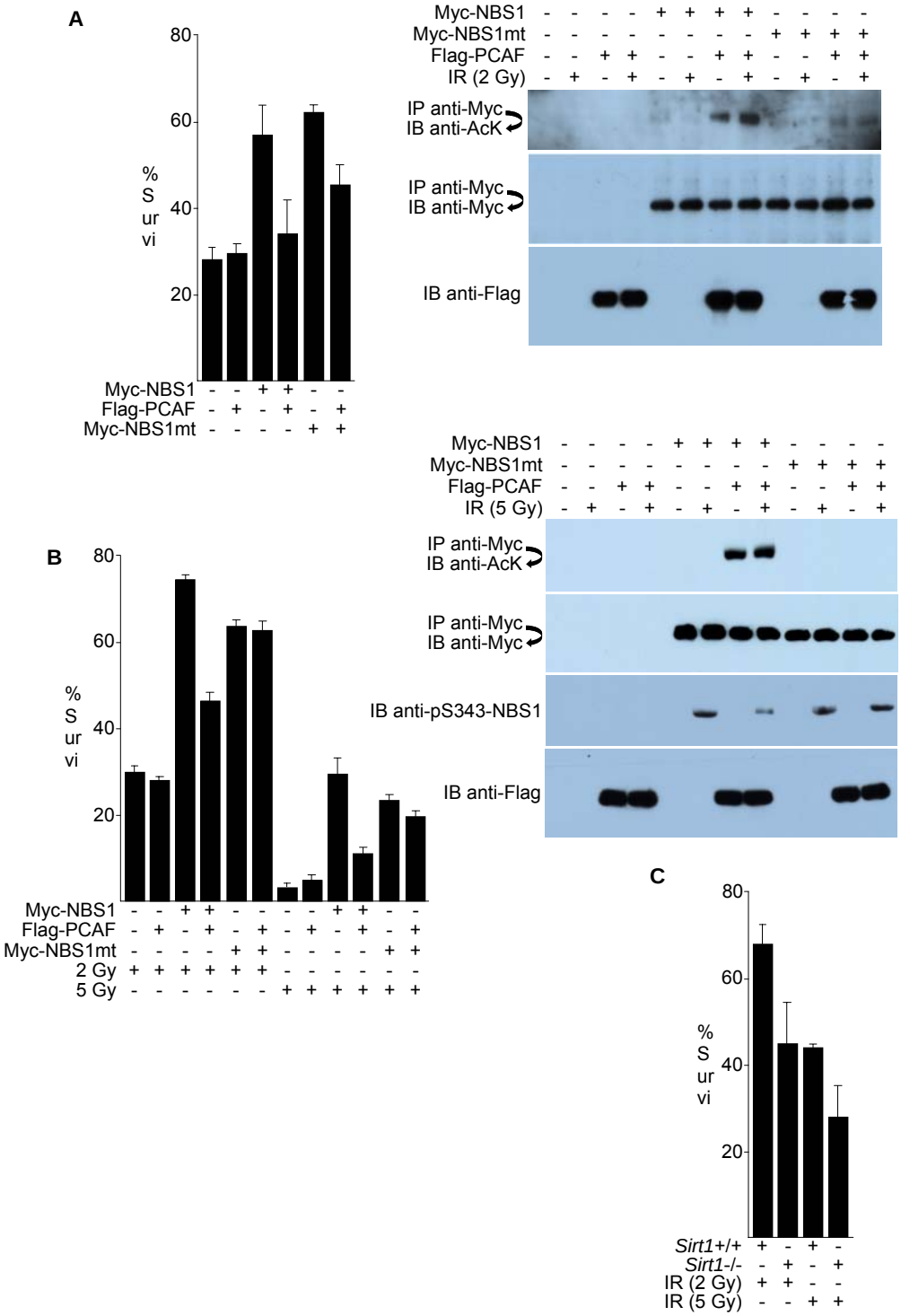

Figure 7. NBS1 Acetylation Affects Cell Survival

Left panel, NBS cells transfected with plasmids (4 ug each) encoding the indicated proteins were irradiated (2 Gy) or left unirradiated. The surviving colonies were counted two weeks later. Right panels, direct Western blots and high

stringency immunoprecipitation/Western blot analyses were performed to determine NBS1 acetylation, immunoprecipitation efficiency, and protein expression levels. Representative blots are shown. (C) *Sirt1*+/+ and *Sirt1*-/- MEFs were irradiated with the indicated dosage or left unirradiated. The surviving colonies were counted two weeks later. Fractional cell survival is the fraction of colonies surviving irradiation divided by the total number of colonies in the unirradiated parallel culture. The data are expressed as mean ± SD from three separate experiments.

cells expressing mutant NBS1, which is less efficiently acetylated by PCAF, was higher compared to cells expressing wild-type NBS1.

To confirm that hyperacetylation of NBS1 negatively affects cell survival, we repeated the colony survival assays in cells stably expressing wild-type or mutant NBS1 and PCAF. As shown in Figure 7B, the presence of PCAF reduced the ability of wild-type NBS1 to increase cell survival after IR treatment in stably transfected NBS cells. Likewise, in complementary experiments, the absence of *Sirt1* decreased survival rate following γ-IR compared to wild-type MEFs (Figure 7C).

Discussion

HATs and HDACs play critical roles in diverse biological functions. In humans, two well-characterized HATs, hGCN5 and TIP60, play important roles in DNA repair (Brand et al., 2001; Ikura et al., 2000). In the current study, we show that NBS1 can be acetylated by PCAF and p300 and that acetylation of NBS1 inhibits Ser343 phosphorylation. At this time, the exact mechanism by which acetylation/deacetylation of NBS1 modulates phosphorylation is unclear. One plausible model is that hypoacetylation of lysines on NBS1 induces an intramolecular structural change in NBS1 that favors phosphorylation. Our data

clearly indicate that NBS1 acetylation results in a decrease in cell survival and an increase in RDS most likely due to decreased NBS1 phosphorylation.

Mass spectrometry analysis of NBS1 indicated that ten of the 70 lysine residues in NBS1 were acetylated. The NBS1 protein possesses three lysine acetylation consensus motifs, $Kx_{1-2}x/KK$, (previously described by Yang, 2004), at residues 233-237 (KGHKK), 683-687 (KNFKK), and 686-690 (KKFKK). However, we found that only two out of the ten potential acetylation sites identified by sequence analysis were actually acetylated (residues 233 and 690). Moreover, eight other acetylation sites detected on NBS1 by mass spectrometry analysis do not conform to any consensuses. Therefore, not only does substrate recognition by SIRT1 not dependent on the amino acid sequence proximate to the acetylated lysine (Blander et al., 2005), it appears that the NBS1 acetyltransferase(s) similarly does not have strict sequence requirements.

Although we cannot rule out the possibility that in addition to p300 and PCAF more acetyltransferases can modify NBS1, our data clearly demonstrate that NBS1 is deacetylated predominantly, if not exclusively, by SIRT1. Our results are consistent with a model in which SIRT1 is required to maintain hypoacetylated NBS1, which promotes efficient IR-induced NBS1 phosphorylation and the ensuing cellular responses to DNA damage. Thus, an additional function of SIRT1 may be to maintain NBS1 in a constant hypoacetylated state. Alternatively, IR may induce SIRT1 activity in order to regulate the acetylation status of NBS1; however, this possibility cannot be tested directly due to the low basal levels of acetylated NBS1. Despite this

dilemma, these results are in accordance with the notion that SIRT1, in addition to silencing transcription, plays an important role in suppressing genomic instability and, consequently, in regulating aging in mammals (Lombard et al., 2005).

Many evidences suggest a close link between histone deacetylation and DNA repair. For example, the yeast Sin3/Rpd3 complex has been shown to modulate DNA DSB repair through the deacetylation of histone H4K16 (Jazayeri et al., 2004). The Sir2 and Rpd3 proteins are recruited to HO lesions during homology-directed repair (Tamburini and Tyler, 2005). *RPD3* and *HOS2* are required for the activation of DNA damage-inducible genes *RNR3* and *HUG1* (Sharma et al., 2007). Furthermore, HDAC4 is recruited to DSBs *in vivo* and, therefore, is implicated in DNA repair in mammalian cells (Kao et al., 2003). Knockdown of HDAC4 expression by RNAi increases radiosensitivity and blocks G2/M checkpoint maintenance. Also, it was reported that the SMRT-HDAC3 complex is involved in cellular recovery from DNA DSBs in mammalian cells (Yu et al., 2006). SMRT and HDAC3 are required for transcriptional repression by Ku70, a subunit of the DNA-PK DSB repair complex.

Although p53 is known to be a substrate for SIRT1 (Luo et al., 2001; Vaziri et al., 2001), the contribution of SIRT1 to p53-mediated DNA damage repair is controversial. While one study suggests that SIRT1 modulates p53-dependent DNA-damage responses (Chen et al., 2005), other reports argue that SIRT1 does not affect p53-mediated biological activities (Kamel et al., 2006; Solomon et al., 2006). More recently, SIRT6 was found to be a chromatin-associated protein

that promotes normal base excision repair but does not play a role in regulating cell cycle checkpoints (Mostoslavsky et al., 2006). Our finding that SIRT1 deacetylates NBS1 and is intimately involved in the regulation of the intra-S-phase checkpoint, coupled with the recent report that DNA damage induces SIRT1 expression (Wang et al., 2006), raises the intriguing possibility that HDACs ensure genomic stability through a variety of mechanisms involving multiple pathways.

In the MRN complex, besides acetylation/deacetylation and phosphorylation of NBS1, the activities and functions of MRE11 are regulated by posttranslational modifications. MRE11 undergoes cell cycle-dependent phosphorylation in response to several genotoxic agents, and this modification requires NBS1 but not ATM (Dong et al., 1999; Yuan et al., 2002). In addition, MRE11 is methylated at arginine residues by PRMT1, and mutation of the arginines severely impairs the exonuclease activity of MRE11 although the mutated protein still forms the MRN complex (Boisvert et al., 2005). In sharp contrast to the hypoacetylation of NBS1, cells containing hypomethylated MRE11 display intra-S-phase DNA damage checkpoint defects. In preliminary studies, we found that MRE11, but not RAD50, is acetylated in the cell (data not shown). Because SIRT1 associates with the entire MRN complex, future studies are warranted to determine whether MRE11, like NBS1, is similarly regulated by SIRT1 and if so, whether acetylation/deacetylation of MRE11 interacts with other MRE11 modifications to ultimately affect the DNA DSB repair pathway.

References

1. Aizawa, H., Hu, S.C., Bobb, K., Balakrishnan, K., Ince, G., Gurevich, I., Cowan, M., and Ghosh, A. (2004). Dendrite development regulated by CREST, a calcium-regulated transcriptional activator. Science *303*, 197-202.
2. Bakkenist, C.J., and Kastan, M.B. (2003). DNA damage activates ATM through intermolecular autophosphorylation and dimer dissociation. Nature *421*, 499-506.
3. Blander, G., and Guarente, L. (2004). The Sir2 family of protein deacetylases. Annu. Rev. Biochem. *73*, 417-435.
4. Blander, G., Olejnik, J., Krzymanska-Olejnik, E., McDonagh, T., Haigis, M., Yaffe, M.B., and Guarente, L. (2005). SIRT1 shows no substrate specificity in vitro. J. Biol. Chem. *280*, 9780-9785.
5. Boisvert, F. M., Dery, U., Masson, J.Y., and Richard, S. (2005). Arginine methylation of MRE11 by PRMT1 is required for DNA damage checkpoint control. Genes Dev. *19*, 671-676.
6. Brand, M., Moggs, J.G., Oulad-Abdelghani, M., Lejeune, F., Dilworth, F.J., Stevenin, J., Almouzni, G., and Tora, L. (2001). UV-damaged DNA-binding protein in the TFTC complex links DNA damage recognition to nucleosome acetylation. EMBO J. *20*, 3187-3196.
7. Brunet, A., Sweeney, L.B., Sturgill, J.F., Chua, K.F., Greer, P.L., Lin, Y., Tran, H., Ross, S.E., Mostoslavsky, R., Cohen, H.Y., et al. (2004). Stress-dependent regulation of FOXO transcription factors by the SIRT1 deacetylase. Science *303*, 2011-2015.

8. Cerosaletti, K., Wright, J., and Concannon, P. (2006). Active role for nibrin in the kinetics of atm activation. Mol. Cell. Biol. *26*, 1691-1699.
9. Chen, W.Y., Wang, D.H., Yen, R.C., Luo,J., Gu, W., and Baylin, S.B. (2005). Tumor suppressor HIC1 directly regulates SIRT1 to modulate p53-dependent DNA-damage responses. Cell *123*, 437-448.
10. Cheng, H.L., Mostoslavsky, R., Saito, S., Manis, J.P., Gu, Y., Patel, P., Bronson, R., Appella, E., Alt, F.W., and Chua, K.F. (2003). Developmental defects and p53 hyperacetylation in Sir2 homolog (SIRT1)-deficient mice. Proc. Natl. Acad. Sci. USA *100*, 10794-10799.
11. Digweed, M., and Sperling, K. (2004). Nijmegen breakage syndrome: clinical manifestation of defective response to DNA double-strand breaks. DNA Repair *3*, 1207-1217.
12. Dong, Z., Zhong, Q., and Chen, P.L. (1999). The Nijmegen breakage syndrome protein is essential for Mre11 phosphorylation upon DNA damage. J. Biol. Chem. *274*, 19513-19516.
13. Gatei, M., Young, D., Cerosaletti, K.M., Desai-Mehta, A., Spring, K., Kozlov, S., Lavin, M.F., Gatti, R.A., Concannon, P., and Khanna, K. (2000). ATM-dependent phosphorylation of nibrin in response to radiation exposure. Nat. Genet. *25*, 115-119.
14. Giannakou, M.E., and Partridge, L. (2004). The interaction between FOXO and SIRT1: tipping the balance towards survival. Trends Cell Biol. *14*, 408-412.

15. Glozak, M.A., Sengupta, N., Zhang, X., and Seto, E. (2005). Acetylation and deacetylation of non-histone proteins. Gene *363*, 15-23.

16. Gray, S.G., and Ekstrom, T.J. (2001). The human histone deacetylase family. Exp. Cell Res. *262*, 75-83.

17. Gregoretti, I.V., Lee, Y.M., and Goodson, H.V. (2004). Molecular evolution of the histone deacetylase family: functional implications of phylogenetic analysis. J. Mol. Biol. *338*, 17-31.

18. Guarente, L. (2006). Sirtuins as potential targets for metabolic syndrome. Nature *444*, 868-874.

19. Haigis, M.C., and Guarente, L.P. (2006). Mammalian sirtuins--emerging roles in physiology, aging, and calorie restriction. Genes Dev. *20*, 2913-2921.

20. Hassig, C.A., and Schreiber, S.L. (1997). Nuclear histone acetylases and deacetylases and transcriptional regulation: HATs off to HDACs. Curr. Opin. Chem. Biol. *1*, 300-308.

21. Ikura, T., Ogryzko, V.V., Grigoriev, M., Groisman, R., Wang, J., Horikoshi, M., Scully, R., Qin, J., and Nakatani, Y. (2000). Involvement of the TIP60 histone acetylase complex in DNA repair and apoptosis. Cell *102*, 463-473.

22. Jazayeri, A., McAinsh, A.D., and Jackson, S.P. (2004). Saccharomyces cerevisiae Sin3p facilitates DNA double-strand break repair. Proc. Natl. Acad. Sci. USA *101*, 1644-1649.

23. Johnson, C.A., and Turner, B.M. (1999). Histone deacetylases: complex transducers of nuclear signals. Semin. Cell Dev. Biol. *10*, 179-188.

24. Kamel, C., Abrol, M., Jardine, K., He, X., and McBurney, M.W. (2006). SirT1 fails to affect p53-mediated biological functions. Aging Cell *5*, 81-88.

25. Kao, G.D., McKenna, W.G., Guenther, M.G., Muschel, R.J., Lazar, M.A., and Yen, T.J. (2003). Histone deacetylase 4 interacts with 53BP1 to mediate the DNA damage response. J. Cell Biol. *160*, 1017-1027.

26. Kobayshi, J., Tauchi, H., Sakamoto, S., Nakamura, A., Morishima, K., Matsuura, S., Kobayashi, T., Tamai, K., Tanimoto, K., and Komatsu, K. (2002). NBS1 localizes to gamma-H2AX foci through interaction with the FHA/BRCT domain. Curr. Biol. *12*, 1846-1851.

27. Kouzarides, T. (2000). Acetylation: a regulatory modification to rival phosphorylation? EMBO J. *19*, 1176-1179.

28. Kuo, M.H., and Allis, C.D. (1998). Roles of histone acetyltransferases and deacetylases in gene regulation. Bioessays *20*, 615-626.

29. Langley, E., Pearson, M., Faretta, M., Bauer, U.M., Frye, R.A., Minucci, S., Pelicci, P.G., and Kouzarides, T. (2002). Human SIR2 deacetylates p53 and antagonizes PML/p53-induced cellular senescence. EMBO J. *21*, 2383-2396.

30. Lee, J.H., and Paull, T.T. (2004). Direct activation of the ATM protein kinase by the Mre11/Rad50/Nbs1 complex. Science *304*, 93-96.

31. Lee, J.H., and Paull, T.T. (2005). ATM activation by DNA double-strand breaks through the Mre11-Rad50-Nbs1 complex. Science *308*, 551-554.

32. Lim, D.S., Kim, S.T., Xu, B., Maser, R.S., Lin, J., Petrini, J.H., and Kastan, M.B. (2000). ATM phosphorylates p95/nbs1 in an S-phase checkpoint pathway. Nature *404*, 613-617.

33. Liszt, G., Ford, E., Kurtev, M., and Guarente, L. (2005). Mouse Sir2 homolog SIRT6 is a nuclear ADP-ribosyltransferase. J. Biol. Chem. *280*, 21313-21320.

34. Lombard, D.B., Chua, K.F., Mostoslavsky, R., Franco, S., Gostissa, M., and Alt, F.W. (2005). DNA repair, genome stability, and aging. Cell *120*, 497-512.

35. Luo, J., Nikolaev, A.Y., Imai, S., Chen, D., Su, F., Shiloh, A., Guarente, L., and Gu, W. (2001). Negative control of p53 by Sir2alpha promotes cell survival under stress. Cell *107*, 137-148.

36. Marks, P.A., Miller, T., and Richon, V.M. (2003). Histone deacetylases. Curr. Opin. Pharmacol. *3*, 344-351.

37. Maser, R.S., Zinkel, R., and Petrini, J.H. (2001). An alternative mode of translation permits production of a variant NBS1 protein from the common Nijmegen breakage syndrome allele. Nat. Genet. *27*, 417-421.

38. Michishita, E., Park, J.Y., Burneskis, J.M., Barrett, J.C., and Horikawa, I. (2005). Evolutionarily conserved and nonconserved cellular localizations and functions of human SIRT proteins. Mol. Biol. Cell *16*, 4623-4635.

39. Mirzoeva, O.K., and Petrini, J.H. (2001). DNA damage-dependent nuclear dynamics of the Mre11 complex. Mol. Cell. Biol. *21*, 281-288.

40. Mostoslavsky, R., Chua, K.F., Lombard, D.B., Pang, W.W., Fischer, M.R., Gellon, L., Liu, P., Mostoslavsky, G., Franco, S., Murphy, M.M., et al. (2006). Genomic instability and aging-like phenotype in the absence of mammalian SIRT6. Cell *124*, 315-329.

41. Nemoto, S., Fergusson, M.M., and Finkel, T. (2005). SIRT1 functionally interacts with the metabolic regulator and transcriptional coactivator PGC-1a. J. Biol. Chem. *280*, 16456-16460.

42. North, B.J., Marshall, B.L., Borra, M.T., Denu, J.M., and Verdin, E. (2003). The human Sir2 ortholog, SIRT2, is an NAD+-dependent tubulin deacetylase. Mol. Cell *11*, 437-444.

43. Peterson, C.L. (2002). HDAC's at work: everyone doing their part. Mol. Cell *9*, 921-922.

44. Rodgers, J.T., Lerin, C., Haas, W., Gygi, S.P., Spiegelman, B.M., and Puigserver, P. (2005). Nutrient control of glucose homeostasis through a complex of PGC-1alpha and SIRT1. Nature *434*, 113-118.

45. Roth, S.Y., Denu, J.M., Allis, C.D. (2001). Histone acetyltransferases. Annu. Rev. Biochem. *70*, 81-120.

46. Ruijter, A.J.M., van Gennip, A.H., Caron, H.N., Kemp, S., and van Kuilenburg, A.B.P. (2003). Histone deacetylases (HDACs): characterization of the classical HDAC family. *370*, 737-749.

47. Shiloh, Y. (1997). Ataxia-telangiectasia and the Nijmegen breakage syndrome: related disorders but genes apart. Annu. Rev. Genet. *31*, 635-662.

48. Solomon, J.M., Pasupuleti, R., Xu, L., McDonagh, T., Curtis, R., DiStefano, P.S., and Huber, L.J. (2006). Inhibition of SIRT1 catalytic activity increases p53 acetylation but does not alter cell survival following DNA damage. Mol. Cell. Biol. *26*, 28-38.

49. Sterner, D.E., and Berger, S.L. (2000). Acetylation of histones and transcription-related factors. Microbiol. Mol. Biol. R. *64*, 435-459.

50. Sui, G., Soohoo, C., Affar el, B., Gay, F., Shi, Y., Forrester, W.C., and Shi, Y. (2002). A DNA vector-based RNAi technology to suppress gene expression in mammalian cells. Proc. Natl. Acad. Sci. USA *99*, 5515-5520.

51. Tamburini, B.A., and Tyler, J.K. (2005). Localized histone acetylation and deacetylation triggered by the homologous recombination pathway of double-strand DNA repair. Mol. Cell. Biol. *25*, 4903-4913.

52. Tauchi, H., Kobayashi, J., Morishima, K., van Gent, D.C., Shiraishi, T., Verkaik, N.S., vanHeems, D., Ito, E., Nakamura, A., Sonoda, E., et al. (2002). Nbs1 is essential for DNA repair by homologous recombination in higher vertebrate cells. Nature *420*, 93-98.

53. Tauchi, H., Matsuura, S., Kobayashi, J., Sakamoto, S., and Komatsu, K. (2002). Nijmegen Breakage Syndrome gene, NBS1, and molecular links to factors for genome stability. Oncogene *21*, 8967-8980.

54. van der Burgt, I., Chrzanowska, K.H., Smeets, D., and Weemaes, C. (1996). Nijmegen breakage syndrome. J. Med. Genet. *33*, 153-156.

55. Vaquero, A., Scher, M., Lee, D., Erdjument-Bromage, H., Tempst, P., and Reinberg, D. (2004). Human SirT1 interacts with histone H1 and promotes formation of facultative heterochromatin. Mol. Cell *16*, 93-105.

56. Vaquero, A., Scher, M.B., Lee, D.H., Sutton, A., Cheng, H.L., Alt, F.W., Serrano, L., Sternglanz, R., and Reinberg, D. (2006). SirT2 is a histone

deacetylase with preference for histone H4 Lys 16 during mitosis. Genes Dev. *20*, 1256-1261.

57. Varon, R., Vissinga, C., Platzer, M., Cerosaletti, K.M., Saar, K., Beckmann, G., Seemanova, E., Cooper, P.R., Nowak, N.J., Stumm, M., et al. (1998). Nibrin, a novel DNA double-strand break repair protein, is mutated in Nijmegen breakage syndrome. Cell *93*, 467-476.
58. Vaziri, H., Dessain, S.K., Ng Eaton, E., Imai, S.I., Frye, R.A., Pandita, T.K., Guarente, L., and Weinberg, R. A. (2001). hSIR2(SIRT1) functions as an NAD-dependent p53 deacetylase. Cell *107*, 149-159.
59. Wang, C., Chen, L., Hou, X., Li, Z., Kabra, N., Ma, Y., Nemoto, S., Finkel, T., Gu, W., Cress, W.D., and Chen, J. (2006). Interactions between E2F1 and SirT1 regulate apoptotic response to DNA damage. Nat. Cell Biol. *8*, 1025-1031.
60. Wolffe, A.P. (1996). Histone deacetylase: a regulator of transcription. Science *272*, 371-372.
61. Wu, X., Ranganathan, V., Weisman, D.S., Heine, W.F., Ciccone, D.N., O'Neill, T.B., Crick, K.E., Pierce, K.A., Lane, W.S., Rathbun, G., et al. (2000). ATM phosphorylation of Nijmegen breakage syndrome protein is required in a DNA damage response. Nature *405*, 477-482.
62. Yang, X.J. (2004). Lysine acetylation and the bromodomain: a new partnership for signaling. Bioessays *26*, 1076-1087.

63. Yang, X.J., Ogryzko, V.V., Nishikawa, J., Howard, B.H., and Nakatani, Y. (1996). A p300/CBP-associated factor that competes with the adenoviral oncoprotein E1A. Nature *382*, 319-324.

64. Yang, X.J., and Seto, E. (2003). Collaborative spirit of histone deacetylases in regulating chromatin structure and gene expression. Curr. Opin. Genet. Dev. *13*, 143-153.

65. You, Z., Chahwan, C., Bailis, J., Hunter, T., and Russell, P. (2005). ATM activation and its recruitment to damaged DNA require binding to the C terminus of Nbs1. Mol. Cell. Biol. *25*, 5363-5379.

66. Yu, J., Palmer, C., Alenghat, T., Li, Y., Kao, G., and Lazar, M.A. (2006). The corepressor silencing mediator for retinoid and thyroid hormone receptor facilitates cellular recovery from DNA double-strand breaks. Cancer Res. *66*, 9316-9322.

67. Yuan, S.S., Su, J.H., Hou, M.F., Yang, F.W., Zhao,S., and Lee, E.Y. (2002). Arsenic-induced Mre11 phosphorylation is cell cycle-dependent and defective in NBS cells. DNA Repair *1*, 137-142.

68. Zhang, Q., Yao, H., Vo, N., and Goodman, R.H. (2000). Acetylation of adenovirus E1A regulates binding of the transcriptional corepressor CtBP. Proc. Natl. Acad. Sci. USA *97*, 14323-14328.

69. Zhang, X., Wharton, W., Yuan, Z., Tsai, S.C., Olashaw, N., and Seto, E. (2004). Activation of the growth-differentiation factor 11 gene by the histone deacetylase (HDAC) inhibitor trichostatin A and repression by HDAC3. Mol. Cell. Biol. *24*, 5106-5118.

70. Zhao, S., Renthal, W., and Lee, E.Y. (2002). Functional analysis of FHA and BRCT domains of NBS1 in chromatin association and DNA damage responses. Nucleic Acids Res. *30*, 4815-4822.

71. Zhao, S., Weng, Y.C., Yuan, S.S., Lin, Y.T., Hsu, H.C., Lin, S.C., Gerbino, E., Song, M.H., Zdzienicka, M.Z., Gatti, R.A., et al. (2000). Functional link between ataxia-telangiectasia and Nijmegen breakage syndrome gene products. Nature *405*, 473-477.

SECTION II

HISTONE DEACETYLASE 9 MODULATES CELL SURVIVAL BY REGULATING THE ATDC-P53 COMPLEX

Abstract

HDAC9 is a class II HDAC that acts as a signal-responsive suppressor of cardiac hypertrophy. Several proteins, most notably the myocyte enhancer-binding factor 2 (MEF2), have been found to partner with HDAC9. Through its interactions with MEF2, HDAC9 represses MEF2 activity. By using immunoaffinity chromatography, we have identified a novel HDAC9-interacting protein, ATDC, the product of the ataxia-telangiectasia group D complementing gene. The ATDC gene was originally isolated on the basis of its ability to complement the ionizing radiation sensitivity defect of AT group D fibroblasts. We found that ATDC is an HDAC9 substrate and its biological functions are finely controlled by HDAC9. ATDC sequesters p53 in the cytoplasm, facilitating cell survival by antagonizing the p53-mediated apoptotic pathway following ionizing radiation. By modulating the acetylation of ATDC, HDAC9 prevents ATDC-p53 complex formation, promoting IR-induced cell death. Importantly, we found that ATDC acetylation may also play important roles in regulating pancreatic and cervical carcinoma radiosensitivity and survival. Thus, our results have important

implications regarding clinical treatment for radio-resistant tumors caused by amplified expression of ATDC.

Introduction

Histone deacetylases (HDACs) are a family of enzymes whose functions have been overwhelmingly associated with gene expression and chromatin dynamics (Hassig and Schreiber, 1997; Kuo and Allis, 1998; Johnson and Turner, 1999; Peterson, 2002). 18 human histone deacetylases that share homology through their deacetylase domains have been characterized, and they may be broadly divided into three classes on the basis of homology to the yeast HDACs RPD3 (class I), HDA1 (class II) and Sir2 (class III) (Gray and Ekstrom, 2001; Yang and Seto, 2003; Ruijter et al., 2003; Gregoretti et al., 2004; Marks et al., 2003). Class I HDACs consist of nuclear proteins that are generally small in size (40-55 kDa) and are ubiquitously expressed. In contrast, Class II HDACs are larger (ranging from 100 to 160 kDa), with expression patterns that tend to be tissue-specific (Ruijter et al., 2003; Marks et al., 2003). Recent studies have implicated the importance of HDACs in normal development and abnormal HDAC expression to have a function in a number of human diseases (Johnstone et al, 2003; Kramer et al., 2001).

The gene encoding the HDAC9 protein is located on chromosome 7p21 (Mahlknecht et al., 2002). The human HDAC9 open reading frame is 3036 bp long and encodes a 1011 a.a. protein with a predicted molecular weight of 111.3 kDa and an isoelectric point of 6.41 (Zhou et al., 2001). The HDAC9 gene

encodes multiple protein isoforms, some of which display distinct cellular localization patterns (Petrie et al., 2003), and HDAC9 could shuttle between cytoplasm and nucleus (Zhou et al., 2001; Zhang et al., 2002). HDAC9 contains a conserved deacetylase domain, represses reporter activity when recruited to a promoter, and utilizes histones H3 and H4 as substrates in vitro and in vivo (Zhou et al., 2001; Petrie et al., 2003). HDAC9 is expressed in a tissue-specific pattern, most highly in heart tissue (Zhou et al., 2001; Zhang et al., 2002; Petrie et al., 2003). It was reported that HDAC9 could restrict cardiac growth in response to stress (Zhang et al., 2002).

The ATDC (ataxia telangiectasia group D complementing) gene was originally identified by its ability to complement the radiosensitivity defect of a cell line (AT5BIVA) from the D complementation group of the autosomal recessive human genetic disease ataxia telangiectasia (AT) (Kapp et al., 1992; Leonhardt et al., 1994). There are multiple zinc finger motifs and an adjacent leucine zipper motif in ATDC (Leonhardt et al., 1994). Endogenous and overexpressed ATDC protein locate in the cytoplasm (Laderoute et al., 1996; Brzoska et al., 1995; Reymond et al., 2001). ATDC gene is significantly amplified in human pancreatic and cervical carcinomas (Iacobuzio-Donahue et al., 2002; Zhang et al. 2005). Although ATDC could complement the radiosensitivity of cells, the underlying mechanisms and its role in tumorigenesis are largely unknown.

In the present study, we found that ATDC is an acetylated protein which is finely controlled by HDAC9. As a cytoplasmic protein, ATDC might facilitate cell survival by sequestering p53 in the cytoplasm and antagonizing the p53-mediated apoptotic pathway following ionizing radiation. By modulating the acetylation of ATDC, HDAC9 could regulate the ATDC-p53 complex formation, promoting IR-induced cell death. Importantly, ATDC acetylation may also play important roles in regulating pancreatic and cervical carcinoma radiosensitivity and survival.

Materials and Methods

Plasmids, Antibodies, and Viruses

The following expression plasmids used in these experiments have been described previously: Flag-HDAC9 (Zhou et al., 2001), Flag-HDAC9 isoforms (Petrie et al., 2003), Flag-PCAF (Yang et al., 1996), HA-p300 (Aizawa et al., 2004), pRc/RSV-HA-CBP (Zhang et al., 2000), pC53-SN3 and BP-100 GL2 (Peng et al., 2003), GST-p53 and its deletion mutants, pGL3 control (Promega). The plasmids encoding HA-ATDC and its deletion mutants were generated by standard PCR and subcloning. HA-ATDC K102R and K116R were generated using the QuickChange Site-Directed Mutagenesis kit following the manufacturer's protocol (Stratagene). HDAC9 shRNA and control shRNA was purchased from openbiosystem. HDAC9 shRNA and control shRNA retroviruses were generated by following the manufacturer's protocol (openbiosystem).

Mouse affinity purified monoclonal anti-Flag M2, rabbit affinity purified polyclonal anti-HA, were purchased from Sigma. Goat polyclonal anti-ATDC, goat polyclonal anti-p53 and mouse monoclonal anti-p53 (clone DO-1) antibodies were purchased from Santa Cruz Biotechnology. Rabbit polyclonal anti-acetyl-lysine was purchased from Upstate (Millipore). Rabbit polyclonal anti-acetylated-Lys382-p53 was purchased from Cell Signaling Technology.

Cell Culture, Transfection, and Adenovirus Infection

293T, HeLa, SiHa were grown in Dulbecco's modified Eagle's medium (DMEM) supplemented with 10% fetal calf serum (FCS) and penicillin/streptomycin (pen/strep). The AT5BIVA cell line (GM05849) was obtained from Coriell Cell Repository and grown in minimum essential medium (MEM) with 10% FCS and pen/strep. All transfections were normalized with equal amounts of parental vector DNA. Transfections were performed with Lipofectamine 2000 (Invitrogen) according to the manufacturer's instructions. For viral infection, HeLa cells were infected with retrovirus for 24 h in DMEM by following the manufacturer's protocol (openbiosystem).

Purification of HDAC9 Containing Complex

HeLa cells were infected with Adenovirus-HA-HDAC9-Flag or Adenovirus-GFP control. Affinity purification of HA- and Flag-tagged HDAC9-containing complex was performed according to previously published method (Rezai-Zadeh et al., 2004). Pufified complexes were concentrated, resolved by SDS-PAGE, and

analyzed by silver staining. A Coomassie blue-stained sample was prepared in parallel, and bands corresponding to HDAC9-associated proteins were excised and subjected to proteolysis with trypsin. Peptides from these mixtures were sequenced by microcapilary LC-MS/MS.

Immunoprecipitation and Western Blot Analysis

For immunoprecipitations, cells were lysed in buffer (50 mM Tris-HCl [pH 7.5], 1 mM EDTA, 1% NP-40, and protease inhibitor cocktail) containing either 500 mM NaCl (high stringency) or 150 mM NaCl (low stringency). The lysates were incubated with the primary antibody overnight at 4^{o}C. The resultant immunocomplexes were collected, washed four times in lysis buffer, and resolved by SDS-PAGE. For immunoblotting, samples were transferred onto nitrocellulose membranes. Membranes were probed with the appropriate antibodies. Proteins of interest were visualized using the Chemiluminescent Detection Kit (Pierce).

Ion Trap Mass Spectrometry

293T cells were transfected with the HA-ATDC expression plasmid and treated with TSA (1.3 M) overnight. The cells were then lysed in high stringency buffer containing 10 mM NaB and 10 mM nicotinamide. Cell extracts were subjected to immunoprecipitation with anti-HA antibodies. The immune complexes were resolved by SDS-PAGE and stained with colloidal Blue (Invitrogen). The HA-ATDC sequence was analyzed with an in-house algorithm (EnzOpt) for a dual

enzyme strategy maximizing proteotypic peptide coverage of all lysines. The appropriate HA-ATDC gel band was excised and divided into two parts. Each part was subjected to in-gel reduction and carboxyamidomethylation followed by separate tryptic or chymotryptic digestion. Acetylated peptides from each digest were detected and sequenced using microcapillary reverse-phase HPLC nano-electrospray tandem mass spectrometry (LC-MS/MS) on a Thermo LTQ linear quadrupole ion trap mass spectrometer. Data analysis was facilitated with SEQUEST and Proteomics Browser Suite (Thermo).

GST Pull-Down Assay

GST and GST-p53 deletion mutants were expressed and purified from bacteria using standard methods. Equimolar quantities of the various purified proteins were conjugated to glutathione-Sepharose beads and incubated with 293T cell (transfected with Flag-ATDC) lysates for 1 h at 4°C. After extensive washing, bound proteins were eluted and analyzed by Western blotting with anti-Flag antibodies.

Colony Survival Assay

Colony survival assays were performed as previously described (Zhao et al., 2002) with minor modifications. Briefly, 24 h after transfection, cells were plated in quadruplicate (1,000 cells per 60-mm tissue culture dish). The cells were γ-irradiated with 0, 2, 2.5 or 7.5Gy as indicated. After two weeks, dishes were washed with PBS, fixed in ice-cold methanol for 15 min, and then stained with

Giemsa stain for 30 min. Colonies on each plate were quantified and expressed as the percentage of the unirradiated control.

Luciferase Assay

Luciferase assay was performed as previously described (Zhang et al., 2004). Briefly, U2OS cells were plated in 6-well dishes at a density of 4 x 10^5 cells/well. 24hr after transfection, cells were treated as indicated in figures before harvesting with 250 µl of passive lysis buffer (Promega). Protein concentrations of all samples were determined using Bradford reagent (Bio-Rad), and the relative light unit values were measured with firefly assay reagent (Promega) and a luminometer.

Immunofluorescence Assay

Cells were washed with PBS, fixed in 4% paraformaldehyde for 10min at room temperature. Cells were permeabilized for 15min at room temperature using 0.5% TritonX-100 in PBS. After blocking by 1% BSA in PBS for 30min, cells were incubated with primary antibody at cold room overnight, followed by Alexa-555 and Alexa-488-conjugated secondary antibody for 1h at room temperature. Wash three times with PBS, dry slides, and mount slides with Bectashield mounting medium with DAPI. Pictures were taken using Zeiss confocal microscopy.

Cell Apoptotic Assay

Cell apoptotic assay was performed as previously described (Sawada et al., 2003) with minor modifications. Briefly, apoptosis was induced by γ-irradiation (5Gy for AT5BIVA cells and 10Gy for U2OS cells). To examine the effects of ATDC or HDAC9, 10^5 cells were cotransfected with 0.1 ug of pEGFP-C3 (GFP expression plasmid, Clonetech) to mark the transfected cells. The vector plasmid of pcDNA3.1 (+) was used as a negative control. One day after transfection, cells were treated with γ-irradiation. Two days after treatment, cells were stained with DAPI and apoptotic nuclei were counted in GFP-expressing cells under a fluorescence microscope (three hundred cells were counted for each experiment). Each point in figures showing percentages of apoptosis represents the mean ±s.e.m of three experiments.

Results

Immunoaffinity Purification of HDAC9 Containing Complex

To further characterization of HDAC9 biological function, we used an epitope-tagging strategy to isolate HDAC9-containing protein complexes from human cells. We generated an adenovirus encoding double-tagged human HDAC9 protein containing N-terminal HA and C-terminal Flag epitopes (HA-HDAC9-Flag) (Figure 8A) using the pAdEasy-1 system (He et al., 1998). To isolate protein complexes containing HDAC9, HeLa cells were infected with Ad-HA-HDAC9-Flag or Adenovirus vector for 36hrs. Whole cellular extracts from the infected

cells were sequentially subjected to affinity chromatography on M2 (Flag antibody) agarose beads and an HA-affinity column. Finally, the bound proteins were fractionated by SDS-PAGE and visualized by silver staining (Figure 8B). A major protein band of 65 kDa was copurified with HDAC9 from HA-HDAC9-Flag-expressing cells (Figure 1B, lane 2 and 4) but not from virus control cells (Figure 8B, lane 1 and 3), suggesting that this protein is a specific binding partner of HDAC9. By peptide sequencing of the band using mass spectrometric analysis, it was identified as a known protein called ATDC (Accession # Q14134).

ATDC Interacts with HDAC9

To confirm the interaction between HDAC9 and ATDC, we cotransfected the Flag-HDAC9 and HA-ATDC plasmids transiently into 293T cells. Cell lysates were subsequently mixed with the anti-HA agarose and the resulting immune complexes were collected and analyzed by immunoblotting with the anti-Flag antibody (Figure 8C). As indicated in Figure 8C, immunoprecipitation of HA-ATDC from lysates of these cotransfected cells resulted in coprecipitation of Flag-HDAC9. We also detected this interaction reciprocally by using the anti-Flag antibody for immunoprecipitation and anti-HA antibody for probing of the blotted precipitate (Figure 8D). These observations provided the first indication that HDAC9 and ATDC can form physical complexes with one another in vivo.

To investigate the interaction between endogenous HDAC9 and ATDC, cell extracts from HeLa cells were immunoprecipitated with anti-ATDC or with the

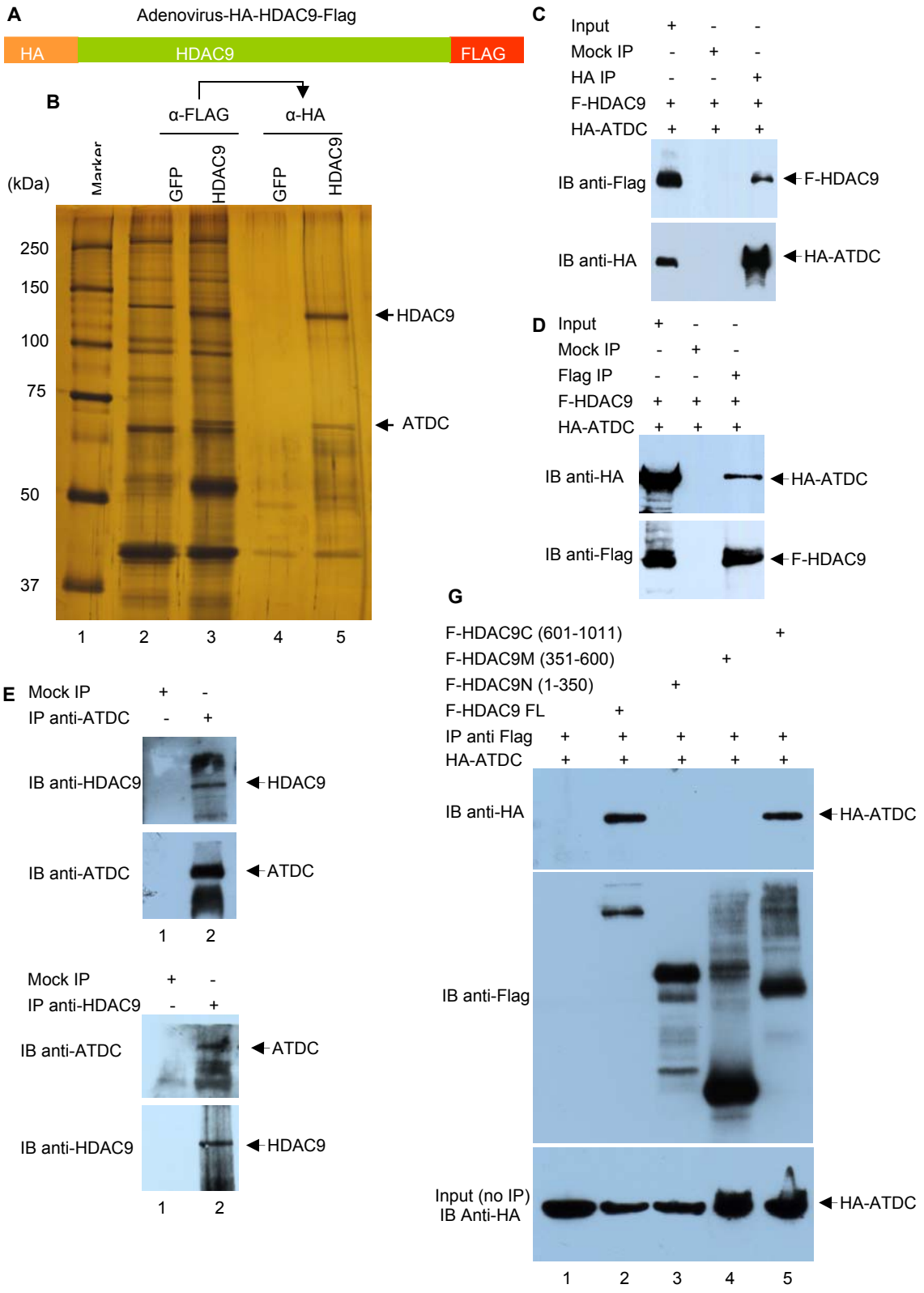
A
Adenovirus-HA-HDAC9-Flag
HA
HDAC9
FLAG
B
α-FLAG
α-HA
(kDa)
Marker
GFP
HDAC9
GFP
HDAC9
250
150
100
75
50
37
HDAC9
ATDC
1
2
3
4
5
C
Input + - -
Mock IP - + -
HA IP - - +
F-HDAC9 + + +
HA-ATDC + + +
IB anti-Flag
F-HDAC9
IB anti-HA
HA-ATDC
D
Input + - -
Mock IP - + -
Flag IP - - +
F-HDAC9 + + +
HA-ATDC + + +
IB anti-HA
HA-ATDC
IB anti-Flag
F-HDAC9
E
Mock IP + -
IP anti-ATDC - +
IB anti-HDAC9
HDAC9
IB anti-ATDC
ATDC
1
2
F
Mock IP + -
IP anti-HDAC9 - +
IB anti-ATDC
ATDC
IB anti-HDAC9
HDAC9
1
2
G
F-HDAC9C (601-1011) +
F-HDAC9M (351-600) +
F-HDAC9N (1-350) +
F-HDAC9 FL +
IP anti Flag + + + + +
HA-ATDC + + + + +
IB anti-HA
HA-ATDC
IB anti-Flag
Input (no IP)
IB Anti-HA
HA-ATDC
1
2
3
4
5

Figure 8. Immuno-affinity purification of HDAC9 containing complex

(A) Scheme of the Adenovirus-HA-HDAC9-Flag. (B) Purification of the HDAC9-containing complexes. HA-FLAG-epitope-tagged HDAC9 was purified from HeLa cells infected with adenovirus expressing HA-HDAC9-FLAG by immunoprecipitation with antibody specific for FLAG (lane 2), followed by antibody specific for HA (lane 4). As a control, mock purification was performed from HeLa cells infected with adenovirus expressing GFP alone (lanes 1 and 3). Specific HDAC9-interacting protein bands were peptide sequenced by mass spectrometry. (C, D) 293T cells were co-transfected with plasmids (4ug each) encoding the indicated HA and Flag fusion proteins. Anti-HA and anti-Flag immunoprecipitates obtained under low stringency conditions were analyzed by Western blotting with the indicated antibodies. (E, F) Endogenous ATDC or HDAC9 were immunoprecipitated from HeLa cell lysates under low stringency conditions with anti-ATDC or anti-HDAC9 polyclonal antibodies. Immune complexes were analyzed by Western blotting with indicated antibodies. (G) 293T cells were co-transfected with HA-ATDC and Flag-HDAC9 or its deletion mutants. Anti-Flag immunoprecipitates obtained under low stringency conditions were analyzed by Western blotting with anti-HA antibody.

control IgG. As expected, Western blot analysis revealed that HDAC9 was clearly detected in the immunoprecipitations obtained with the anti-ATDC antiserum (Figure 8E) but not the control IgG (Figure 8E). Conversely, endogenous ATDC was readily immunoprecipitated with the HDAC9-specific antibody (Figure 8F), but not with a control IgG (Figure 8F). These data indicate that HDAC9 and ATDC could form a physical complex in vivo.

To further investigate how ATDC interacts with HDAC9, we generated several HDAC9 deletion mutants. HA-ATDC and Flag-HDAC9 deletion mutants were cotransfected into 293T cells. Cell lysates were immunoprecipitated with anti-flag agarose. As shown in Figure 8G, ATDC specifically bound to HDAC9 C-terminal domain (HDAC9 601-1011aa) (Figure 8G), but not to Flag vector control, the N-terminal domain of HDAC9 (1-350aa) and the central domain (HDAC9 351-600). Thus, the above findings demonstrate that ATDC interacts with mammalian HDAC9 deacetylase in vivo.

ATDC is an Acetylated Protein

Since HDAC9 could form physical complexes with ATDC, we sought to determine whether ATDC could serve as a substrate of HDAC9 enzyme. Firstly, we examined whether ATDC could be modified by acetylation. 293T cells were transfected with the plasmid encoding HA-ATDC. 24hrs post transfection, cells were incubated with ethanol carrier or HDAC chemical inhibitors trichostatin (TSA) overnight. We then immunoprecipitated HA-ATDC from these cells and analyzed the immune complex by western blotting using an antibody previously shown to recognize acetylated lysines in viarious proteins. As shown in figure 9A, treatment with TSA significantly enhances ATDC acetylation. Anti-acetyl-lysine Western blot analysis of anti-ATDC immunoprecipitates revealed that TSA also could enhance the acetylation state of endogenous ATDC (Figure 9B). To map the ATDC lysine-acetylation sites induced by TSA, tandem mass spectrometry analysis was performed. We found that at least 9 lysine sites of ATDC was acetylated (Figure 9C). These data strongly sugested that ATDC was an acetylated protein within cells.

ATDC Acetylation is Regulated by HDAC9

It is well known that the histone acetyltransferases PCAF and p300 target nonhistone proteins for acetylation (Glozak et al., 2005; Kouzarides, 2000; Yang, 2004). So, we co-transfected 293T cells with vectors expressing HA-ATDC and Flag-PCAF or HA-P300. The cell lysates were then analyzed by immunoprecipitation using anti-HA agarose followed by western blotting using

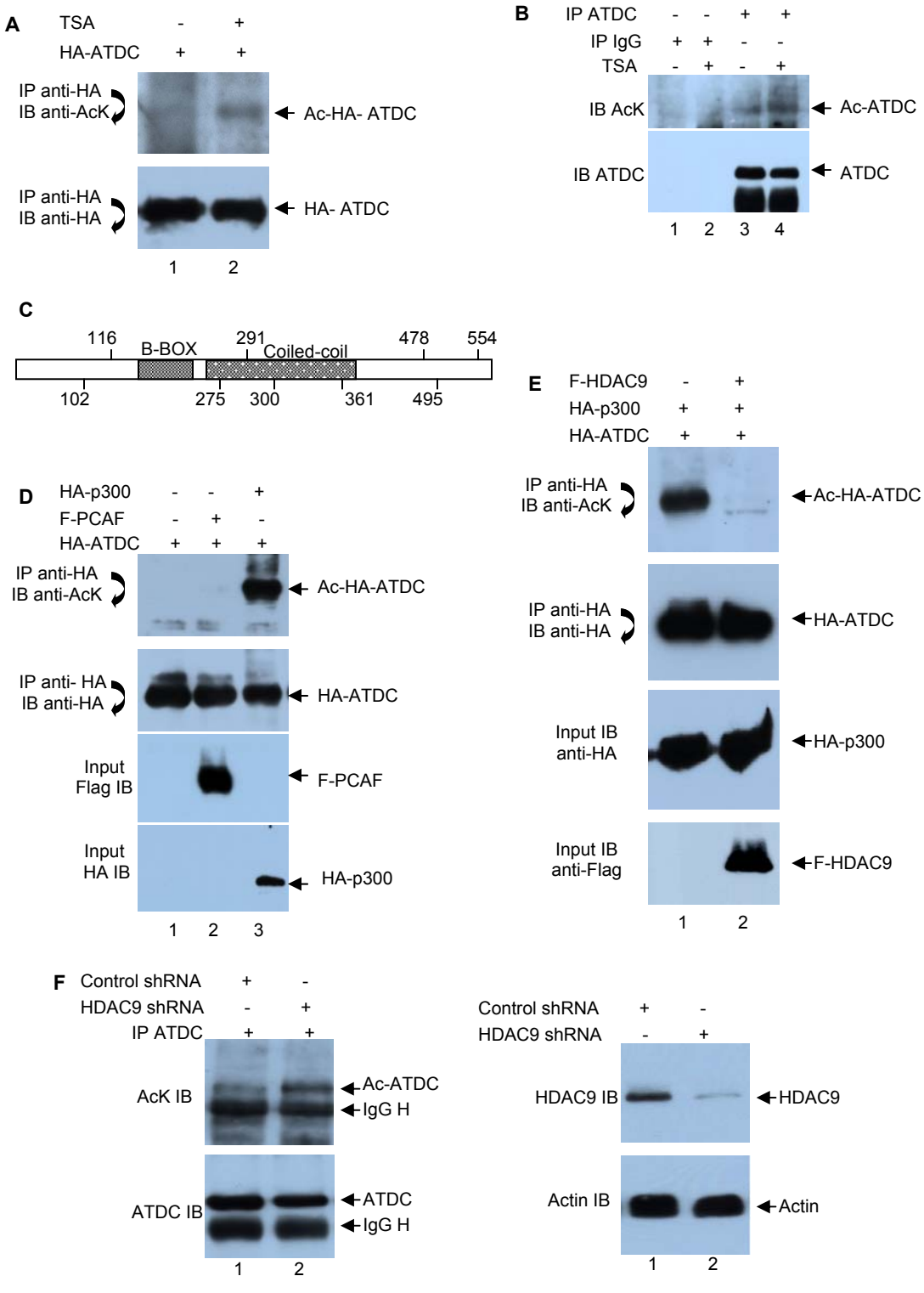
A
TSA - +
HA-ATDC + +
IP anti-HA
IB anti-AcK
Ac-HA- ATDC
IP anti-HA
IB anti-HA
HA- ATDC
1 2
B
IP ATDC - - + +
IP IgG + + - -
TSA - + - +
IB AcK
Ac-ATDC
IB ATDC
ATDC
1 2 3 4
C
116
B-BOX
291
Coiled-coil
478
554
102
275
300
361
495
D
HA-p300 - - +
F-PCAF - + -
HA-ATDC + + +
IP anti-HA
IB anti-AcK
Ac-HA-ATDC
IP anti- HA
IB anti-HA
HA-ATDC
Input
Flag IB
F-PCAF
Input
HA IB
HA-p300
1 2 3
E
F-HDAC9 - +
HA-p300 + +
HA-ATDC + +
IP anti-HA
IB anti-AcK
Ac-HA-ATDC
IP anti-HA
IB anti-HA
HA-ATDC
Input IB
anti-HA
HA-p300
Input IB
anti-Flag
F-HDAC9
1 2
F
Control shRNA + -
HDAC9 shRNA - +
IP ATDC + +
AcK IB
Ac-ATDC
IgG H
ATDC IB
ATDC
IgG H
1 2
Control shRNA + -
HDAC9 shRNA - +
HDAC9 IB
HDAC9
Actin IB
Actin
1 2

Figure 9. ATDC is an acetylated protein which is regulated by HDAC9

(A) 293T cells were transfected with plasmids that expressed HA-ATDC (4ug). Twenty-four hours post-transfection, cells were left untreated or treated overnight with TSA (1.3uM). Cell lysates were subjected to immunoprecipitation/Western blotting. (B) HeLa cells were treated with TSA (1.3uM) or left untreated overnight. Cell lysates were then immunoprecipitated under high stringency conditions with anti-ATDC antibodies. Endogenous acetylated ATDC was analyzed by Western blotting with a mixture of polyclonal anti-acetyl-lysine antibodies. (C) HA-ATDC, which was expressed and purified from 293T cells, was digested with trypsin and subjected to ITMS. Positions of the unambiguously-identified acetylated lysine residues are shown. (D) 293T cells were co-transfected with equal amounts (4ug) of HA-ATDC ± one of the following expression plasmids: Flag-PCAF, or HA-p300. Cell lysates were immunoprecipitated (IP) under high stringency conditions using anti-HA antibodies. Immunoprecipitates were subjected to Western blot (IB) analysis using anti-acetyl-lysine (AcK) antibodies. The blot was stripped and re-probed with anti-HA antibodies to confirm equal immunoprecipitation efficiency and loading. Flag-PCAF and HA-P300 expression were detected in the cell lysate. (E) 293T cells were co-transfected with plasmids that express HA-ATDC, HA-P300, and either a vector or a Flag-HDAC9. Acetylation of HA-ATDC and all protein levels were determined with direct Western blotting or immunoprecipitations followed by Western blotting using the indicated antibodies. (F) HeLa cells were infected with either retrovirus that expresses control siRNA or retrovirus that expresses HDAC9 shRNA. Western blots were performed with the indicated antibodies to assess the acetylation of endogenous ATDC and ATDC immunoprecipitation efficiency. Bottom two panels, western blot to show that HDAC9 shRNA is functional.

anti-acetyl lysine antibody. Acetylated ATDC was readily detected with co-expression of P300, but not with PCAF acetyltransferase (Figure 9D). We found ATDC also could interact with p300 within cells (data not shown).

To further address ATDC acetylation was regulated by HDAC9, we transfected 293T cells with HA-ATDC, P300 and Flag vector or Flag-HDAC9. HA-ATDC was immunoprecipitated and followed by anti-acetyl lysine western blotting. As shown in figure 9E, a high level of acetylated ATDC was found in the cells cotransfected with P300 and HA-ATDC (Figure 9E, lane 1); however, p300-mediated ATDC acetylation levels were significantly decreased by expression of Flag-HDAC9 (Figure 9E, lane 2). Furthermore, we assessed the ATDC

acetylation in HDAC9 knock-down cells by immunoprecipitating endogenous ATDC and immunoblotting with antibodies to acetylated lysine (Figure 9F). Acetylation of endogenous ATDC was enhanced in HDAC9 knock-down cells compared to control shRNA cells (Figure 9F), suggesting that endogenous HDAC9 does influence ATDC acetylation in vivo. As indicated in Figure 9F, endogenous HDAC9 protein levels were reduced by the sequence-specific HDAC9 shRNA but not by control shRNA (Figure 9F, bottom panel). Taken together, these data implicate a strong ATDC deacetylation activity of HDAC9 deacetylase. Acetylation of ATDC was barely detectable in the absence of HDAC9 inhibiotr TSA or exogenous acetyltransferase p300 (Figure 9A and 9D), possibly owing to the limiting amounts of endogenous p300 acetytransferase activity, or ATDC preferentially forming a stable complex with the HDAC9 deacetylase.

HDAC9 has multiple isoforms (Petrie et al., 2003). To test whether ATDC has HDAC9 isoform preference binding capability, 293T cells were cotransfected with the plasmids encoding HA-ATDC and Flag-tagged all known HDAC9 isoforms (Petrie et al., 2003). Cell lysates were immunoprecipitated with anti-flag agarose, and then analyzed with anti-HA antibody. As shown in figure 10A, ATDC preferentially bound to HDAC9-PNAS, and weakly bound to HDAC9ΔE7, but not the other HDAC9 isofroms. Correlated with the binding preference, deacetylation of ATDC by HDAC9 might be also highly isoform-specific since only HDAC9-PNAS shows strong deacetylase activity to ATDC (Figure 10B, lane

2), but not other HDAC9 isoforms we tested (HDAC9ΔE7 or HDAC9-JBC) (Figure 10B, lane 3 and 4).

HDAC7 and HDAC9 were further subdivided into the class IIa HDAC based on their homology (Gray et al., 2001). As indicated in figure 10C, the ATDC-HDAC9 interaction might also be highly HDAC specific since HDAC7 did not co-precipitate with ATDC under identical conditions (Figure 10C). Furthermore, p300-acetylated ATDC was specifically deacetylated by HDAC9 (Figure 10D, lane 3), but not by HDAC7 (Figure 10D, lane 2).

HDAC9 Negatively Regulates ATDC Biological Function

ATDC was cloned and coined by its ability to complement the radiosensitivity defect of the AT5BIVA fibroblast cell line. To observe the effect of HDAC9 on its function, AT5BIVA cells were transfected with vector alone, HA-ATDC alone, Flag-HDAC9 alone or HA-ATDC and Flag-HDAC9 expression constructs. As expected, cell colony survival assay suggested ATDC could complement the AT5BIVA cell radiosensitivity defect (Figure 11A, compare column 1 and 3). Interestingly, HDAC9 coexpression significantly antagonize the ATDC function, with about 25.00% of the cell survival compared with about 47.00% of ATDC alone-complemented cells (Figure 11A, compare column 3 and 4).

It has been reported that γ-irradiation could induce cell apoptosis to a greater extent in AT5BIVA cells than in control fibroblast cell lines (Zhang et al., 2001; Jung et al., 1998). Combining the fact that ATDC could provide AT5BIVA

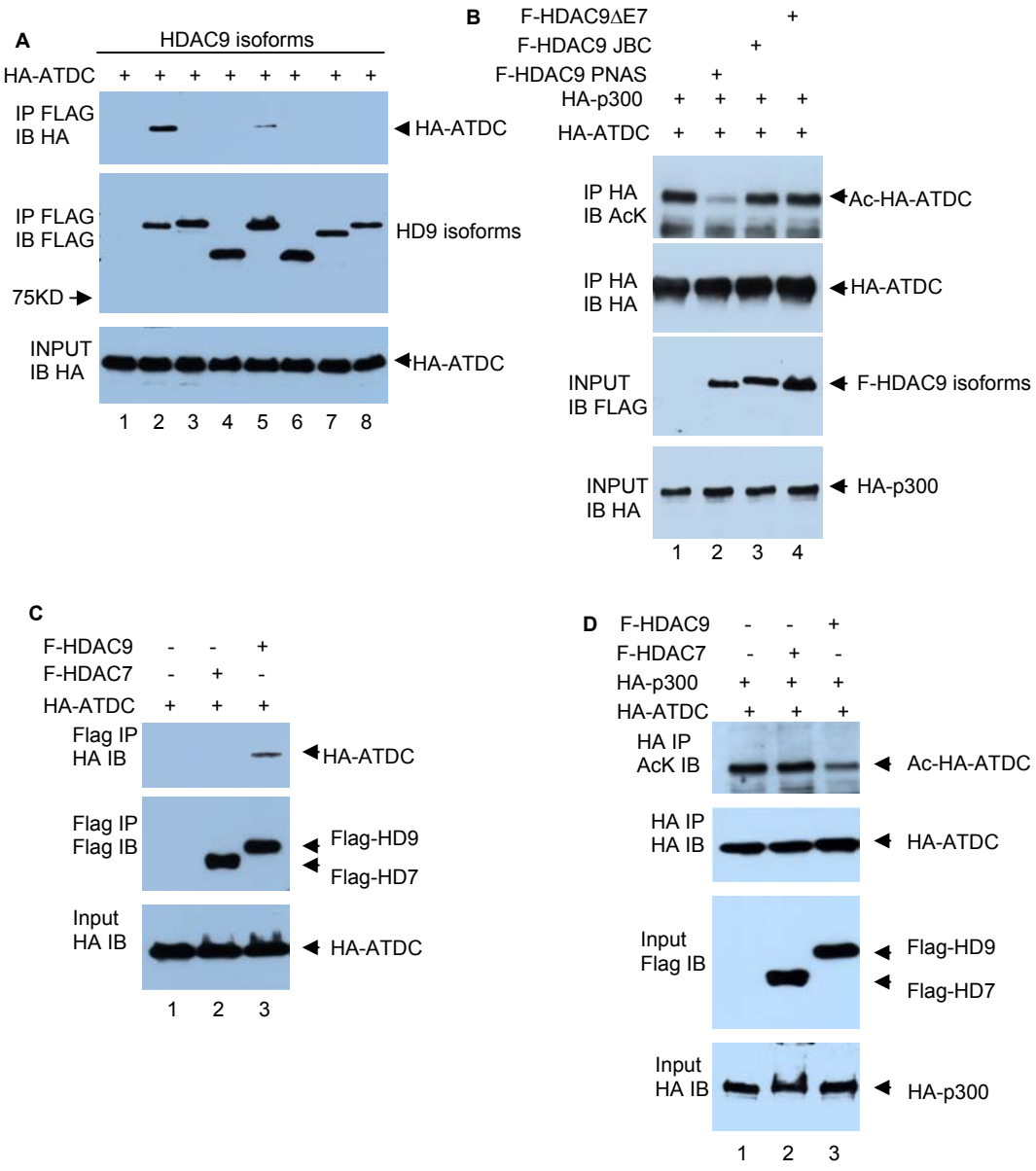

Figure 10. ATDC acetylation is preferentially regulated by HDAC9

(A, C) 293T cells were co-transfected with plasmids (4ug each) encoding the indicated HA and Flag fusion proteins. Anti-HA and anti-Flag immunoprecipitates obtained under low stringency conditions were analyzed by Western blotting with the indicated antibodies. HDAC9 isoforms used in panel A: 1. Vector Control; 2. HDAC9-PNAS; 3. HDAC9-JBC; 4. HDAC9ΔCD; 5. HDAC9ΔE7; 6. HDAC9ΔCDΔE7; 7. HDAC9ΔE12; 8. HDAC9ΔE15. HDAC9-PNAS represents the first reported-HDAC9 gene product on PNAS in 2001, and this is the one we used to purify the HDAC9 containing complex. HDAC9-JBC represents the longest HDAC9 isoform published on JBC in 2003. (B, D) 293T cells were co-transfected with equal amounts (4ug) of HA-ATDC ± the HA-p300 expression plasmid. Cell lysates were immunoprecipitated (IP) under high stringency conditions using anti-HA antibodies. Immunoprecipitates were subjected to Western blot (IB) analysis

using anti-acetyl-lysine (AcK) antibodies. The blot was stripped and re-probed with anti-HA antibodies to confirm equal immunoprecipitation efficiency and loading. HA-P300 and HDACs expression were detected in the cell lysate.

cells a radioresistant phenotype (Kapp et al., 1992; Hosoi et al., 1994), it's interesting to hypothesize that ATDC might facilitate AT5BIVA cell survival by inhibiting γ-irradiation induced-cell death. To test this idea, apoptosis assay was carried out in AT5BIVA cells by expressing vector alone, HA-ATDC alone, Flag-HDAC9 alone or HA-ATDC and Flag-HDAC9. As shown in figure 11B, ATDC significantly decreases the IR-induced AT5BIVA cell apoptosis (Figure 11B, compare column 1 and 3). However, introduction of HDAC9 could strongly reverse the ATDC anti-apoptotic function (Figure 11B, compare column 3 and 4). A parallel western blot shows HDAC9 does not affect the HA-ATDC expression in cells (Figure 11A, right panel).

ATDC Antagonizes p53-mediated Apoptotic Pathway Activated by γ-irradiation and Forms a Physical Complex with p53

P53 has been shown to be important for γ-irradiation-induced apoptosis (Lee et al., 2001; Herzog et al., 1998; Chong et al., 2000). Next, we examined the effect of ATDC on p53-mediated apoptotic pathway. As indicated in figure 12A, ATDC transfected-U2OS (wild type p53+/+) cells were more resistant to γ-irradiation induced-cell death, with about 22.3% of the cells apoptosis while the vector control-transfected cells showed significantly susceptible to apoptosis under the same conditions (Figure 12A, compare column 1 and 2). Furthermore, the same

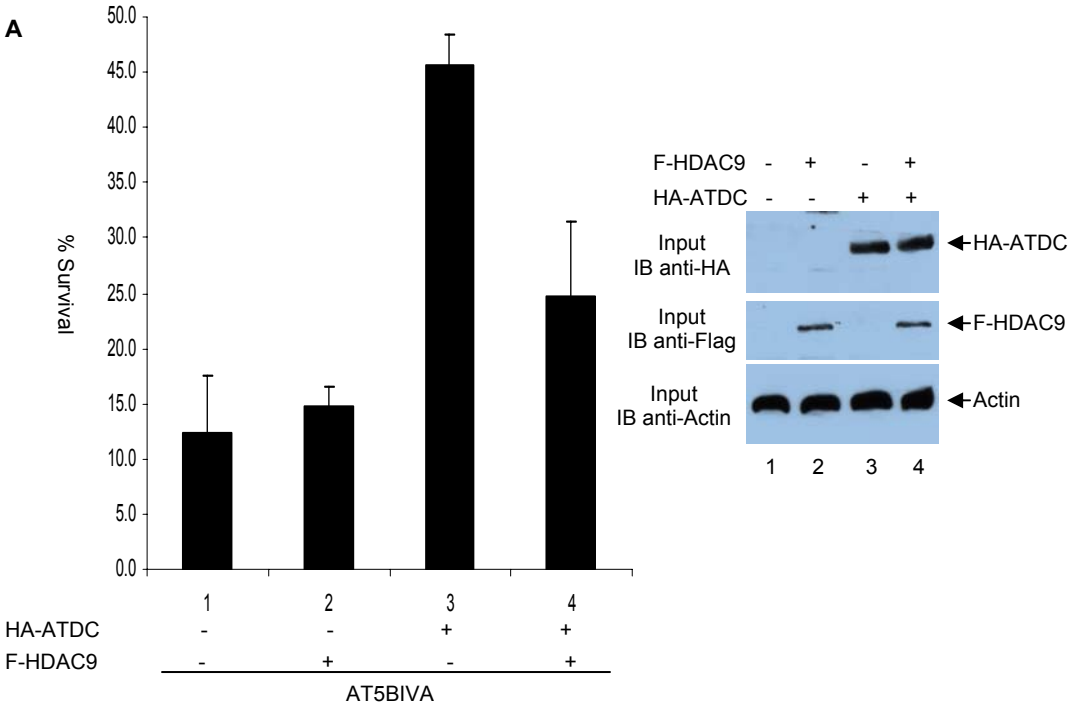
A
% Survival
50.0
45.0
40.0
35.0
30.0
25.0
20.0
15.0
10.0
5.0
0.0
1
2
3
4
HA-ATDC
-
-
+
+
F-HDAC9
-
+
-
+
AT5BIVA
F-HDAC9 - + - +
HA-ATDC - - + +
Input
IB anti-HA
HA-ATDC
Input
IB anti-Flag
F-HDAC9
Input
IB anti-Actin
Actin
1 2 3 4

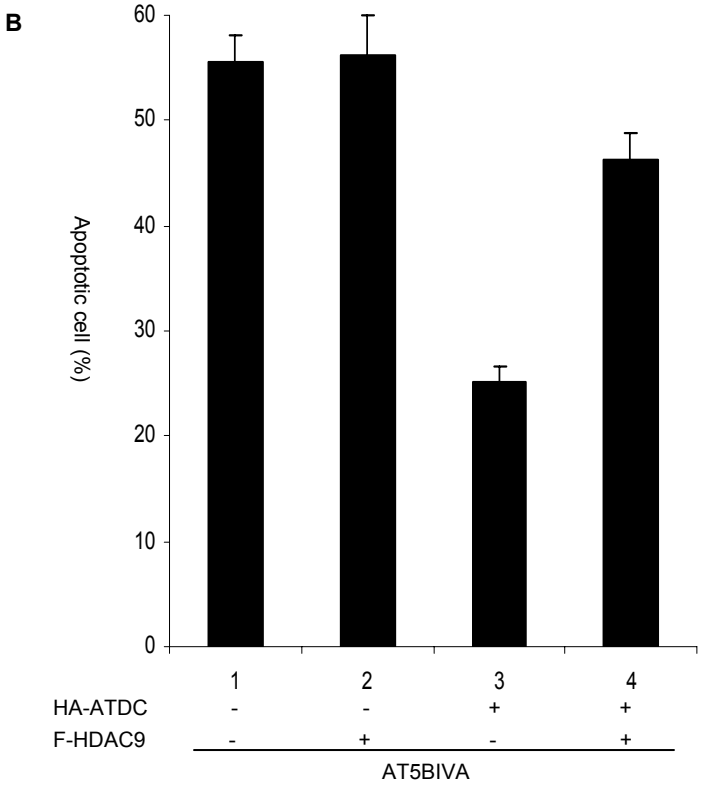
B
Apoptotic cell (%)
60
50
40
30
20
10
0
1
2
3
4
HA-ATDC
-
-
+
+
F-HDAC9
-
+
-
+
AT5BIVA

Figure 11. HDAC9 negatively regulates ATDC biological function

(A) Left panel, AT5BIVA cells transfected with plasmids (4ug each) encoding the indicated proteins were irradiated (2Gy) or left unirradiated. The surviving colonies were counted two weeks later. Right panels, direct Western blots were performed to determine protein expression levels. Representative blots are shown. (B) AT5BIVA cells were transfected as indicated (see Methods). One day after transfection, cells were irradiated (10Gy). After a further 48h, the number of apoptotic cells was counted in GFP+ cells.

experiments were performed in the human p53 null cell line H1299. No significant effect was observed on H1299 cells (Figure 12A, compare column 3 and 4). These data suggested that ATDC could facilitate cell survival by antagonizing the p53-mediated apoptotic pathway activated by γ-irradiation.

To further explore the molecular mechanism by which ATDC affects p53 function, we tested whether ATDC interacts with p53 in vivo. 293T cells (wild type p53+/+) were transfected with HA-ATDC plasmid. Cell lysates were subsequently mixed with the anti-HA agarose and the resulting immune complexes were collected and analyzed by immunoblotting with the p53-specific monoclonal antibody (DO-1) (Figure 12B). As shown in figure 12B, immunoprecipitation of HA-ATDC from lysates of these transfected cells resulted in coprecipitation of endogenous p53. However, γ-irradiation doesn't affect the ATDC-p53 complex formation. These observations provided the first indication that ATDC and p53 can form physical complexes with one another in vivo. This association of ATDC and p53 also occurs in the absence of overexpression, epitope tagging of either protein in SiHa cells (Figure 12C), which express both endogenous ATDC and wild-type

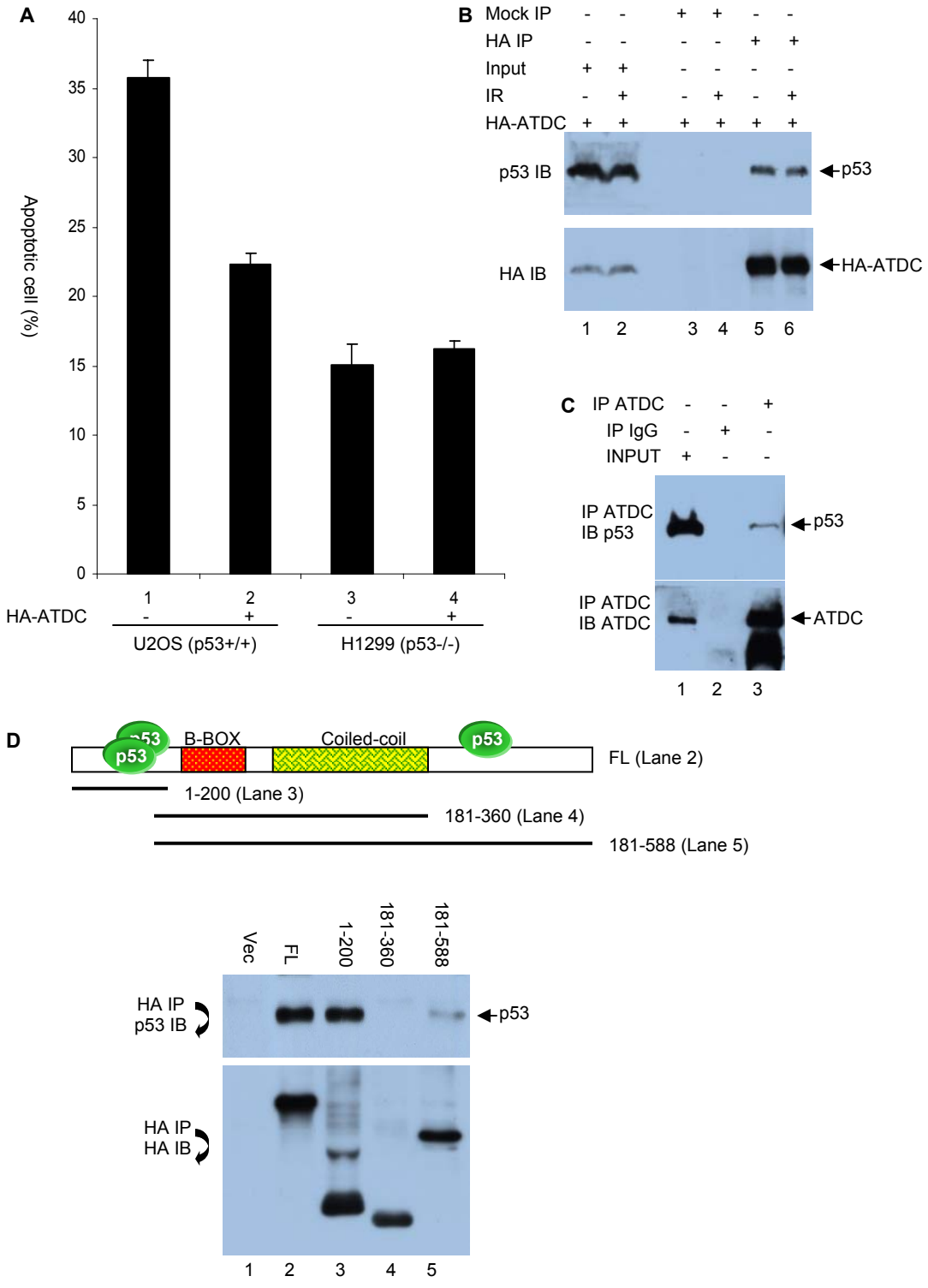
A
Apoptotic cell (%)
40
35
30
25
20
15
10
5
0
1
2
3
4
HA-ATDC
-
+
-
+
U2OS (p53+/+)
H1299 (p53-/-)
B
Mock IP
HA IP
Input
IR
HA-ATDC
p53 IB
HA IB
p53
HA-ATDC
1 2 3 4 5 6
C
IP ATDC
IP IgG
INPUT
IP ATDC
IB p53
IP ATDC
IB ATDC
p53
ATDC
1 2 3
D
p53
B-BOX
Coiled-coil
p53
FL (Lane 2)
1-200 (Lane 3)
181-360 (Lane 4)
181-588 (Lane 5)
Vec
FL
1-200
181-360
181-588
HA IP
p53 IB
HA IP
HA IB
p53
1 2 3 4 5

Figure 12. ATDC facilitates cell survival by antagonizing p53-mediated apoptotic pathway activated by g-irradiation and ATDC forms a physical complex with p53

(A) U2OS and H1299 cells were transfected as indicated (see Methods). One day after transfection, cells were irradiated (10Gy). After a further 48h, the number of apoptotic cells was counted in GFP+ cells. (B) 293T cells were transfected with HA-ATDC. 24hrs post transfection, cells were irradiated (10Gy) or left untreated. One hour after irradiation, HA-ATDC was immunoprecipitated under low stringency conditions with anti-HA agarose. Immune complexes were analyzed by Western blotting with p53 antibody DO-1. (C) Endogenous ATDC was immunoprecipitated from SiHa cell lysates under low stringency conditions with goat anti-ATDC polyclonal antibodies. Immune complexes were analyzed by Western blotting with p53 antibody DO-1. (D) 293T cells were transfected with HA-ATDC or its deletion mutants. Anti-HA immunoprecipitates obtained under low stringency conditions were analyzed by Western blotting with p53 antibody DO-1.

p53 proteins. Analyses of three different HA-ATDC deletions indicated that p53 preferentially interacts with the N-terminus of ATDC (residues 1-200) (Figure 12D).

ATDC Inhibit p53 Function by Sequestering p53 into the Cytoplasm

ATDC mainly located in the cytoplasm (Laderoute et al., 1996; Brzoska et al., 1995; Reymond et al., 2001). To further confirm the ATDC subcellular localization, U2OS cells were transfected with the plasmid encoding HA-ATDC, and immunofluorescence study was carried out. Consistent with the previous findings (Brzoska et al., 1995; Reymond et al., 2001), HA-ATDC was found in the cytoplasm in a ribbon-like structure (Figure 13A). Endogenous ATDC was also found in the cytoplasm in SiHa cells (Figure 13B) and pancreatic carcinoma tissues (Figure 13C). Since ATDC involves in regulating p53-mediated apoptotic pathway, it's intriguing to test whether ATDC directly controls subcellular localization of p53. To test this idea, U2OS cells were transfected with HA-ATDC.

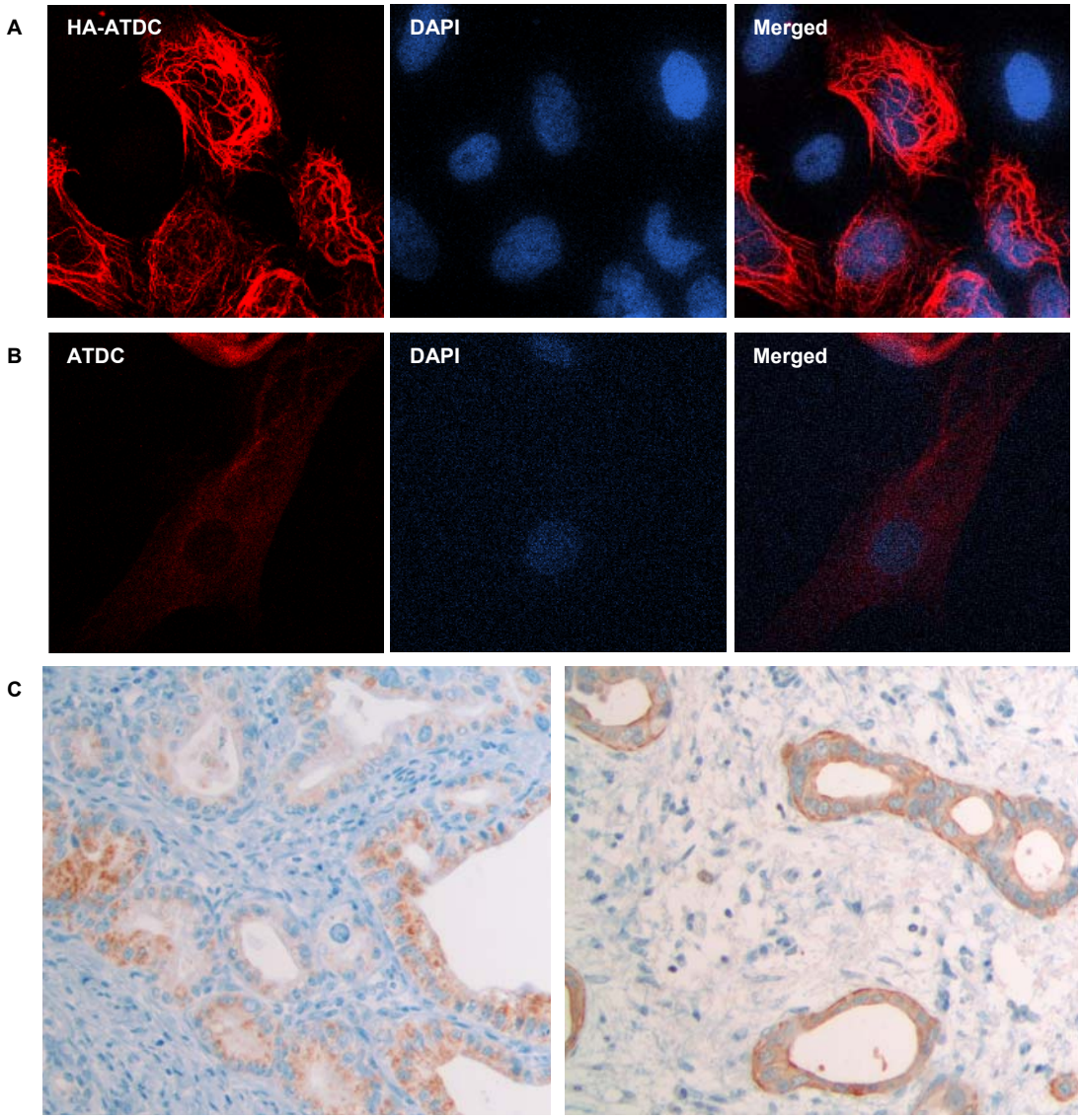

Figure 13. ATDC is a cytoplasmic protein

(A) U2OS cells were transfected with HA-ATDC. 24hr post transfection, cells were fixed, permeabilized, and immunostained with anti-HA antibody. (B) SiHa cells were fixed, permeabilized, and immunostained with anti-ATDC antibody, followed by Alexa-555 secondary antibody. (C) Pancreatic carcinoma tissue samples were stained with anti-ATDC antibody.

As shown by immunofluorescence staining with the p53-specific antibody DO-1 (Figure 14A, inset), p53 mainly located in the nucleus in the absence of overexpressed-ATDC. Strikingly however, after overexpression of ATDC, p53

was predominantly relocalized to the cytoplasm of these cells and displayed a similar pattern as ATDC (Figure 14A). Similar results were also obtained in the cells treated with γ-irradiation (Figure 14A, bottom panel). These data indicated that forced-expression of ATDC could control p53 subcellular localization even under stress. To test the effect of ATDC on endogenous p53 transcriptional activity, U2OS cells were transfected with the p53-responsive BP100-luciferase reporter and different dosage of plasmid encoding HA-ATDC. P53 transcription function was measured by luciferase assay. As shown in figure 14B, ATDC shows strong inhibition of endogenous p53 transcriptional activity (Figure 14B) in a dose dependent manner. The inhibitory effect of ATDC on p53 responsive promoter is quite specific, since the pGL3 control reporter was not affected by ATDC. ATDC even shows similar strong inhibitory effect on p53 transcriptional activity under stress response (Figure 14C).

HDAC9 Regulates the ATDC-p53 Complex Formation and Function

Since ATDC is a HDAC9 substrate as an acetylated protein, it is interesting to address whether HDAC9 could regulate the ATDC-p53 complex formation. To test this idea, 293T cells were transfected with vector, HA-ATDC alone or HA-ATDC and Flag-HDAC9. The cell lysates were immunprecipitated with anti-HA agarose and the resulting immune complexes were collected and analyzed by immunoblotting with the goat anti-p53 polyclonal antibody. Consistent with the above results, ATDC could efficiently pull-down endogenous p53 (Figure 15A, lane 2). However, HDAC9 could significantly inhibit the ATDC and p53 interaction

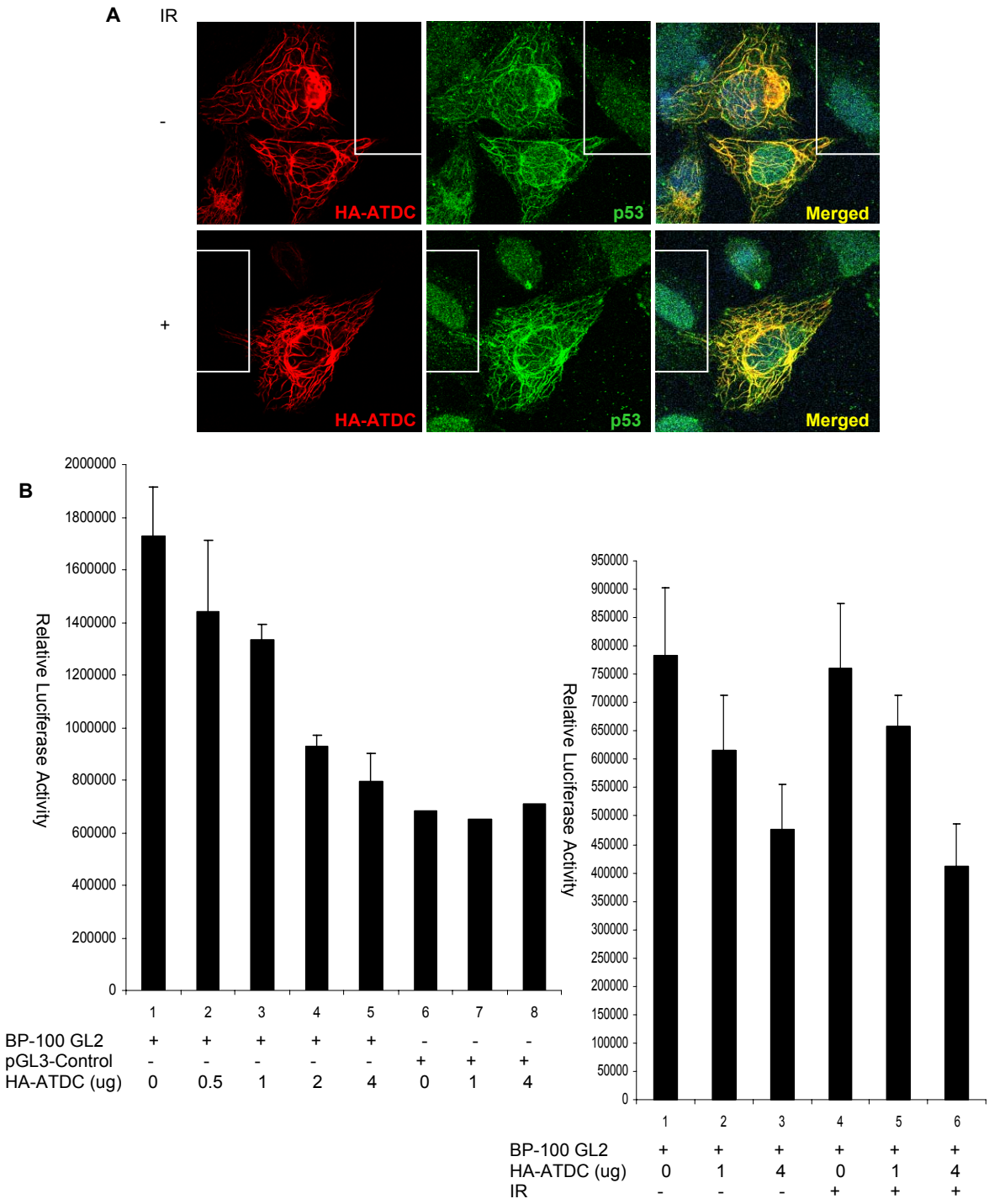

Figure 14. ATDC inhibits p53 function

(A) U2OS cells were transfected with HA-ATDC. 24hr post transfection, cells were left untreated or treated with 10Gy γ-irradiationn. 1hr after treatment, cells were fixed, permeabilized, and stained with anti-HA and anti-p53 DO-1 antibody, followed by Alexa-555 and Alexa-488-conjugated secondary antibodies. Samples were analyzed using Zeiss Confocal

Microscopy. (B) U2OS cells were transfected as indicated. Luciferase activities were determined in triplicate. Error bars show standard deviations. (C) U2OS cells were transfected as indicated. 24hr post transfection, cells were left untreated or treated with 10Gy γ-irradiation. 4hr after treatment, cells were harvested and luciferase activities were determined in triplicate. Error bars show standard deviations.

(Figure 15A, compare lane 3 and 2). Further, treatment with HDAC inhibitor TSA could significantly enhance the ATDC-p53 complex formation (Figure 15B, compare lane 2 and 3). These data suggested that acetylated form of ATDC preferentially interacts with p53 in cells.

Correlated with the above results, TSA treatment could significantly increase the ATDC suppressive effect on endogenous p53 transcriptional activity (Figure 15C). Furthermore, expression of p21, a major transcriptional target of p53, was significantly induced by ATDC-specific siRNA (Figure 15D, left panel) or by overexpression of HDAC9 (Figure 15D, right panel) in SiHa cells although the total level of p53 was unchanged.

ATDC K116 Acetylation is the Major Functional Acetylation Site Responsible for Regulating p53 Interaction

Two acetylation sites of ATDC (K102 and K116) located in the p53 binding domain (ATDC 1-200aa) (Figure 9C and 12D). By aligning the protein sequence among several known vertebrates ATDC homologous (human, chimpanzee, mouse, rat and dog) (Figure 16A), we found that lysine 102 was replaced by arginine in mouse and rat ATDC. Since arginine mutation could mimic the non-acetylated form of lysine (Chan et al., 2001), this suggests K102 acetylation

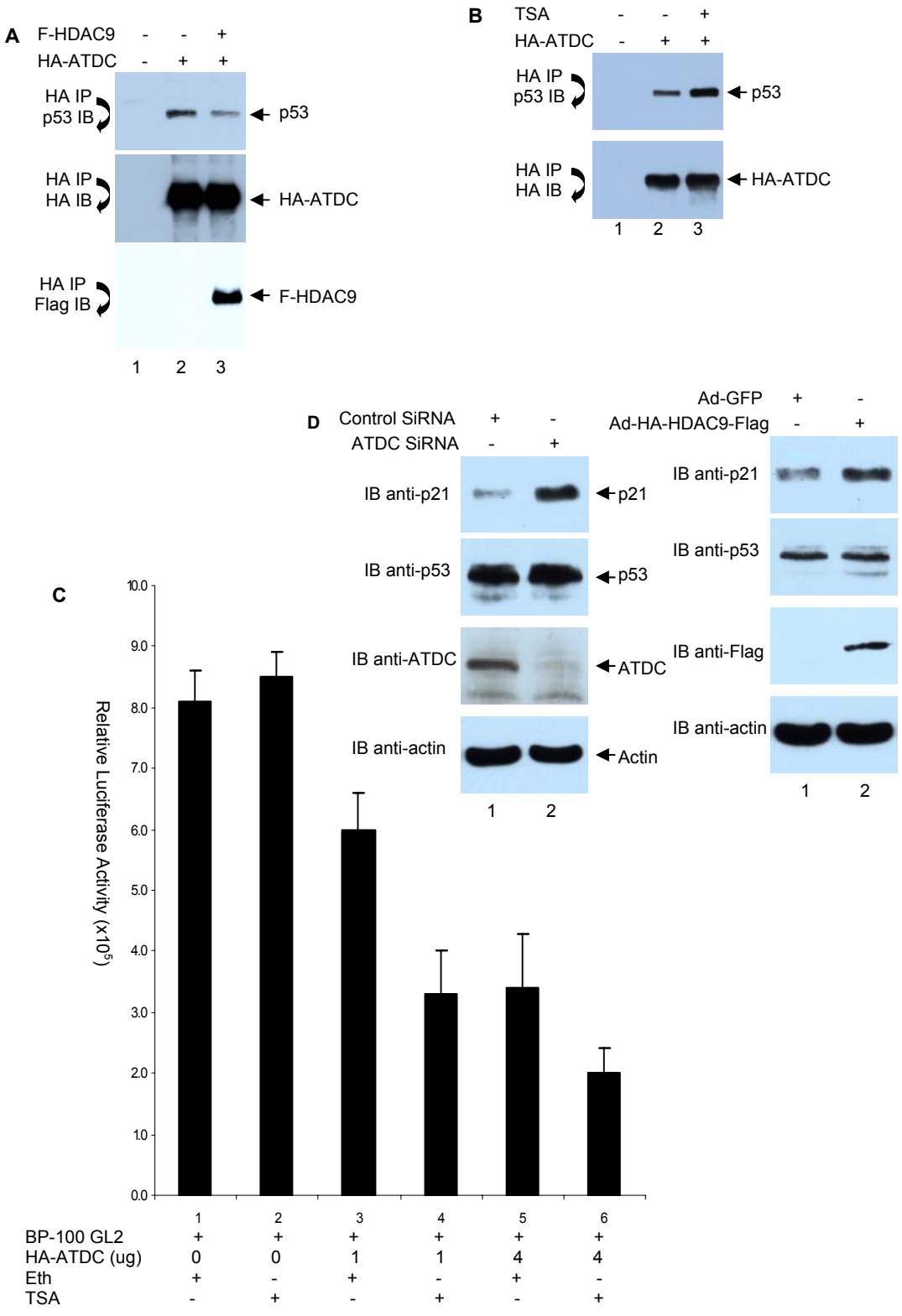
A
F-HDAC9 - - +
HA-ATDC - + +
HA IP
p53 IB
p53
HA IP
HA IB
HA-ATDC
HA IP
Flag IB
F-HDAC9
1 2 3
B
TSA - - +
HA-ATDC - + +
HA IP
p53 IB
p53
HA IP
HA IB
HA-ATDC
1 2 3
C
Relative Luciferase Activity (x10^5)
10.0
9.0
8.0
7.0
6.0
5.0
4.0
3.0
2.0
1.0
0.0
1 2 3 4 5 6
BP-100 GL2 + + + + + +
HA-ATDC (ug) 0 0 1 1 4 4
Eth + - + - + -
TSA - + - + - +
D
Control SiRNA + -
ATDC SiRNA - +
IB anti-p21
p21
IB anti-p53
p53
IB anti-ATDC
ATDC
IB anti-actin
Actin
1 2
Ad-GFP + -
Ad-HA-HDAC9-Flag - +
IB anti-p21
IB anti-p53
IB anti-Flag
IB anti-actin
1 2

Figure 15. HDAC9 regulates the ATDC-p53 complex

(A) 293T cells were co-transfected with HA-ATDC and Flag-HDAC9 or control vector. Anti-HA immunoprecipitates obtained under low stringency conditions were analyzed by Western blotting with p53 antibody DO-1 and anti-Flag. (B) 293T cells were transfected with HA-ATDC. 24hr post transfection, cells were treated with 1.3uM TSA overnight. Anti-HA immunoprecipitates obtained under low stringency conditions were analyzed by Western blotting with p53 antibody DO-1. (C) U2OS cells were transfected as indicated. 24hr post transfection, cells were treated with ethanol carrier or 1.3uM TSA overnight. Cells were harvested and luciferase activities were determined in triplicate. Error bars show standard deviations. (D) U2OS cells were transfected or infected as indicated. 48hr post transfection or infection, cells were harvested, and cell lysates were analyzed as indicated.

might not play an important role in regulating ATDC function. However, K116 in ATDC was quite well conserved, suggesting it might be an important functional acetylation site. To test this idea, human ATDC K102 and K116 were mutated to arginine, individually. As shown in figure 16, mutating lysine 116 to argine significantly decrease ATDC-p53 complex formation and p53 cytoplasm sequestration (Figure 16B). However, there is no effect by mutating human lysine 102 to arginine. Further, K116R mutant could abolish the ATDC inhibitory effect on p53 transcriptional activity (Figure 16C). Interestingly, K116R mutant also abolish the ability of ATDC to complement the radiosensitivity of AT5BIVA cells, but not by K102R mutant (Figure 16D). These data suggested that ATDC biological function was dynamically controlled through K116 acetylation. However, the function of other acetylation sites of ATDC is still not understood yet.

ATDC was Overexpressed in Pancreatic and Cervical Carcinoma

It was reported that mRNA of ATDC was significantly amplified in pancreatic carcinoma and cervical carcinoma (Iacobuzio-Donahue et al., 2002; Zhang et al.

A

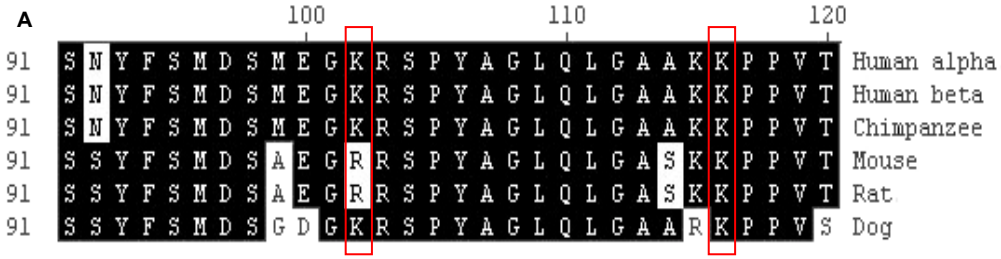
100
110
120
91 S N Y F S M D S M E G K R S P Y A G L Q L G A A K K P P V T Human alpha
91 S N Y F S M D S M E G K R S P Y A G L Q L G A A K K P P V T Human beta
91 S N Y F S M D S M E G K R S P Y A G L Q L G A A K K P P V T Chimpanzee
91 S S Y F S M D S A E G R R S P Y A G L Q L G A S K K P P V T Mouse
91 S S Y F S M D S A E G R R S P Y A G L Q L G A S K K P P V T Rat
91 S S Y F S M D S G D G K R S P Y A G L Q L G A A R K P P V S Dog

B

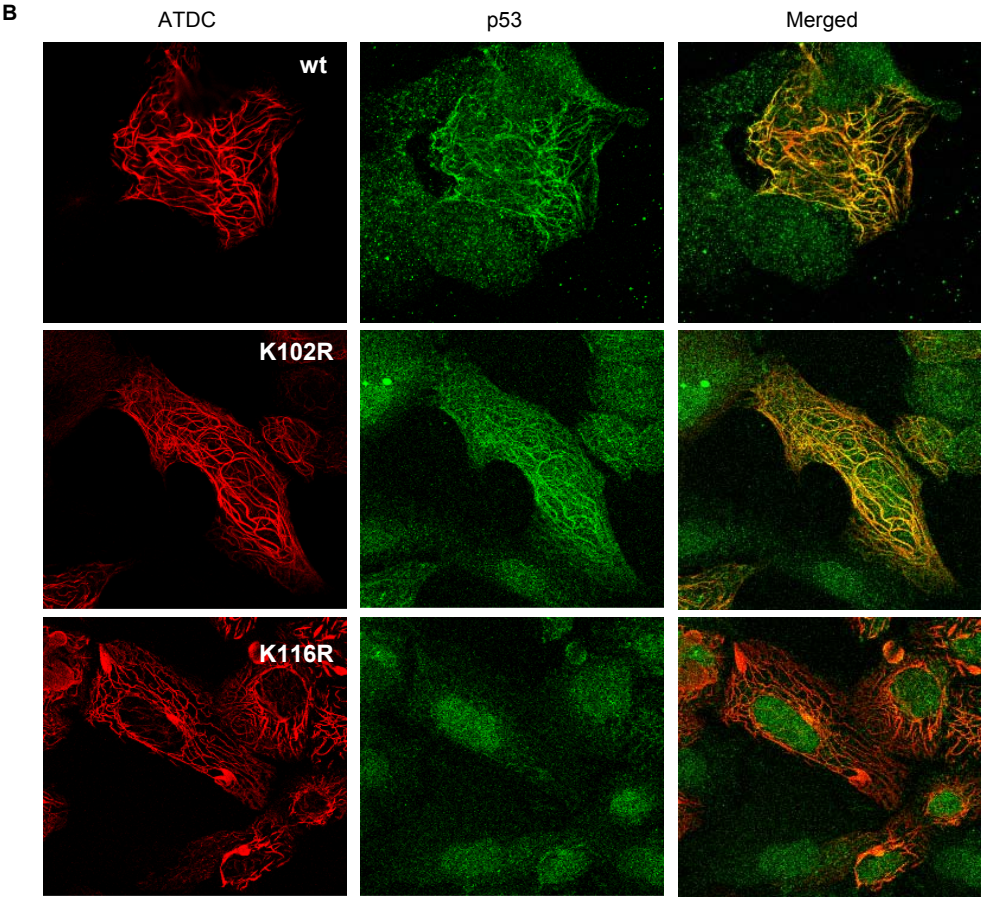
ATDC
p53
Merged
wt
K102R
K116R

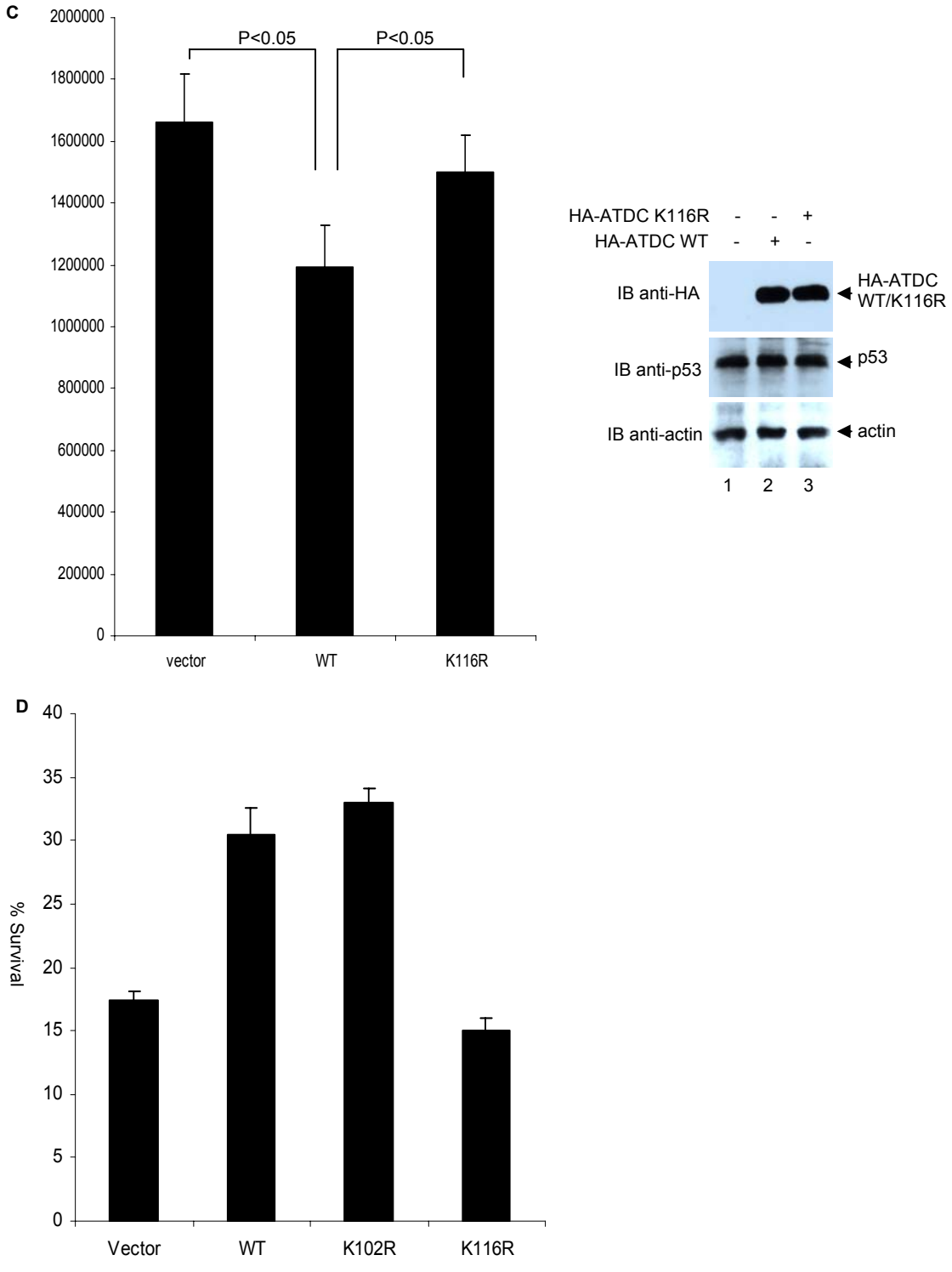

Figure 16. ATDC K116 acetylation play a major role in regulating ATDC-p53 interaction

(A) Alignment of ATDC homologous including human, chimpanzee, mouse, rat and dog. (B) U2OS cells were transfected as indicated. 36hr post transfection, cells were fixed, permeabilized, and stained with anti-HA and anti-p53 DO-1 antibody,

followed by Alexa-555 and Alexa-488-conjugated secondary antibodies. Samples were analyzed using Zeiss Confocal Microscopy. (C) U2OS cells were transfected as indicated. 36hr post transfection, cells were harvested and luciferase activities were determined in triplicate. Error bars show standard deviations. Statistical analysis was done by student t test. Fractions of lysates were analyzed by western blot to check protein expression. (D) AT5BIVA cells transfected with plasmids (4ug each) encoding the indicated proteins were irradiated (2Gy) or left unirradiated. The surviving colonies were counted two weeks later.

2005). As previous shown in figure 13C, ATDC protein is also highly expressed in pancreatic carcinoma tissue. Similarly, the ATDC protein is also highly expressed in the pancreatic carcinoma cell lines that we tested, including Hs766T and BxPC3, and cervical carcinoma cell lines including HeLa and SiHa (Figure 17A) compared to other tumor cell lines. By immunostaining study, we found endogenous ATDC colocalized with endogenous p53 in the cytoplasm in SiHa cell line (wild-type p53+/+) (Figure 17B). Nevertheless, RNAi-mediated reduction of endogenous ATDC leads to nuclear localization of p53 in SiHa cells (Figure 17C). Fruthermore, we tested whether shRNA-mediated inhibition of ATDC function could radio-sensitize cervical carcinomal cells. As indicated in figure 17D, native SiHa cervical carcinoma cells responded poorly to treatment with γ-irradiation. However, treatment with ATDC shRNA significantly makes the cells more susceptible to irradiation treatment. SiHa cells were also sensitized by overexpression of HDAC9, probably through antagonizing the endogenous ATDC function. Furthermore, shRNA-mediated reduction of ATDC and forced-expression of HDAC9 have an additive effect on SiHa cell radiosensitivity when treated with high dosage of γ-irradiation (7.5Gy) (Figure 17D). Thus, the combination of knocking-down ATDC expression and introduction of HDAC9

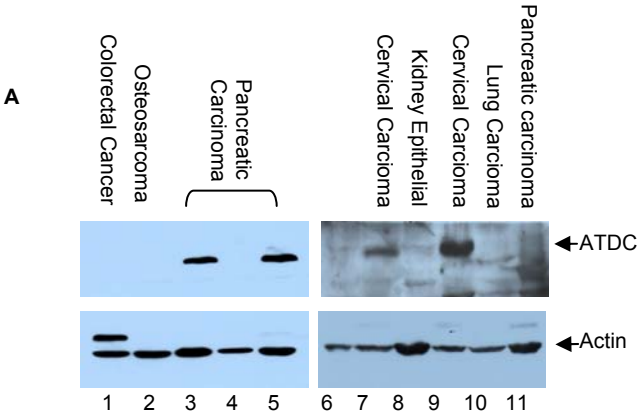
A
Colorectal Cancer
Osteosarcoma
Pancreatic Carcinoma
Cervical Carcioma
Kidney Epithelial
Cervical Carcioma
Lung Carcioma
Pancreatic carcinoma
ATDC
Actin
1 2 3 4 5 6 7 8 9 10 11

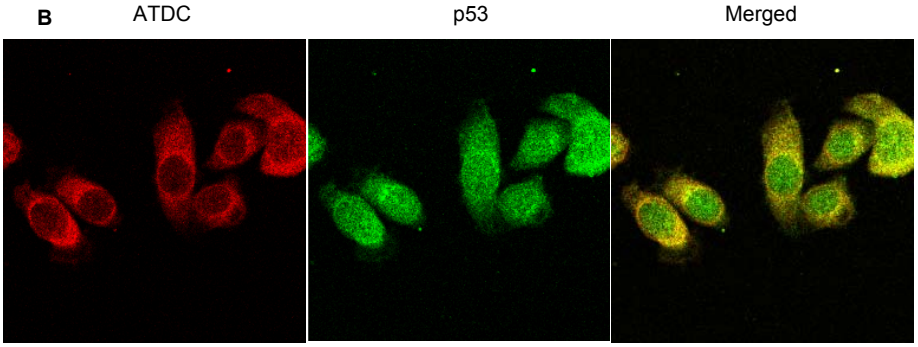
B
ATDC
p53
Merged

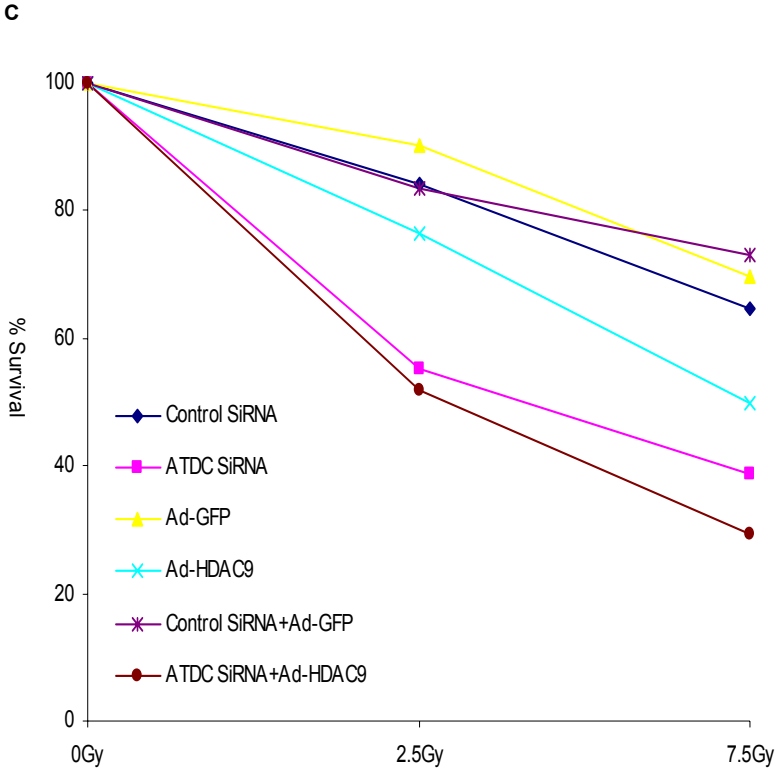
C
100
80
60
40
20
0
% Survival
Control SiRNA
ATDC SiRNA
Ad-GFP
Ad-HDAC9
Control SiRNA+Ad-GFP
ATDC SiRNA+Ad-HDAC9
0Gy
2.5Gy
7.5Gy

Figure 17. Endogenous ATDC in cervical carcinoma cells regulates p53 nuclear localization and function

(A) ATDC is highly expressed in pancreatic and cervical carcinoma cell lines. Whole-cell extracts of different cell lines were immunoblotted with anti-ATDC antibody (upper) and anti-actin antibody (lower). (1.HCT116; 2. U2OS; 3. Hs766T; 4. CAPAN-2; 5. Bx-PC3; 6. AT5BIVA; 7. HeLa; 8. 293T; 9. SiHa; 10. A549; 11. COLO357). (B) SiHa cells were fixed, permeabilized, and stained with anti-ATDC and anti-p53 DO-1 antibodies, followed by Alexa-555 and Alexa-488-conjugated secondary antibodies, and analyzed using Zeiss Confocal Microscopy. (C) SiHa cells were transfected with control or ATDC siRNA. 48 hr post transfection, cells were fixed, permeabilized, and stained with anti-ATDC and anti-p53 DO-1 antibodies, followed by Alexa-555 and Alexa-488-conjugated secondary antibodies, and analyzed using Zeiss Confocal Microscopy. (D) SiHa cells transfected or infected as indicated. 48hr post transfection or infection, cells were irradiated (2.5 or 7.5Gy) or left unirradiated. The surviving colonies were counted 10 days later.

might be an alternative treatment for the radio-resistant tumors caused by amplified ATDC expression.

Growth Stress Induce ATDC Acetylation

Since ATDC plays an important role in regulating p53-mediated apoptotic pathway and might have a significant effect on the clinical radio-therapy for tumors, it is tempting to identify the physiological conditions under which ATDC are highly acetylated in cells. We treated cervical carcinoma cells with various extracellular stimuli and performed Western blot experiments with antibodies to acetylated lysine. As shown in figure 18A and 18B, acetylation of endogenous ATDC in HeLa cells is dynamically inducible in response to growth factors stimulation including EGF (Figure 18A) and PMA (Figure 18B). In contrast, ATDC acetylation was not affected by γ-irradiation (data not shown). Thus, ATDC acetylation appears to be specifically induced in response to growth stress stimuli. Similar results were obtained in SiHa cells treated with PMA (Figure 18C).

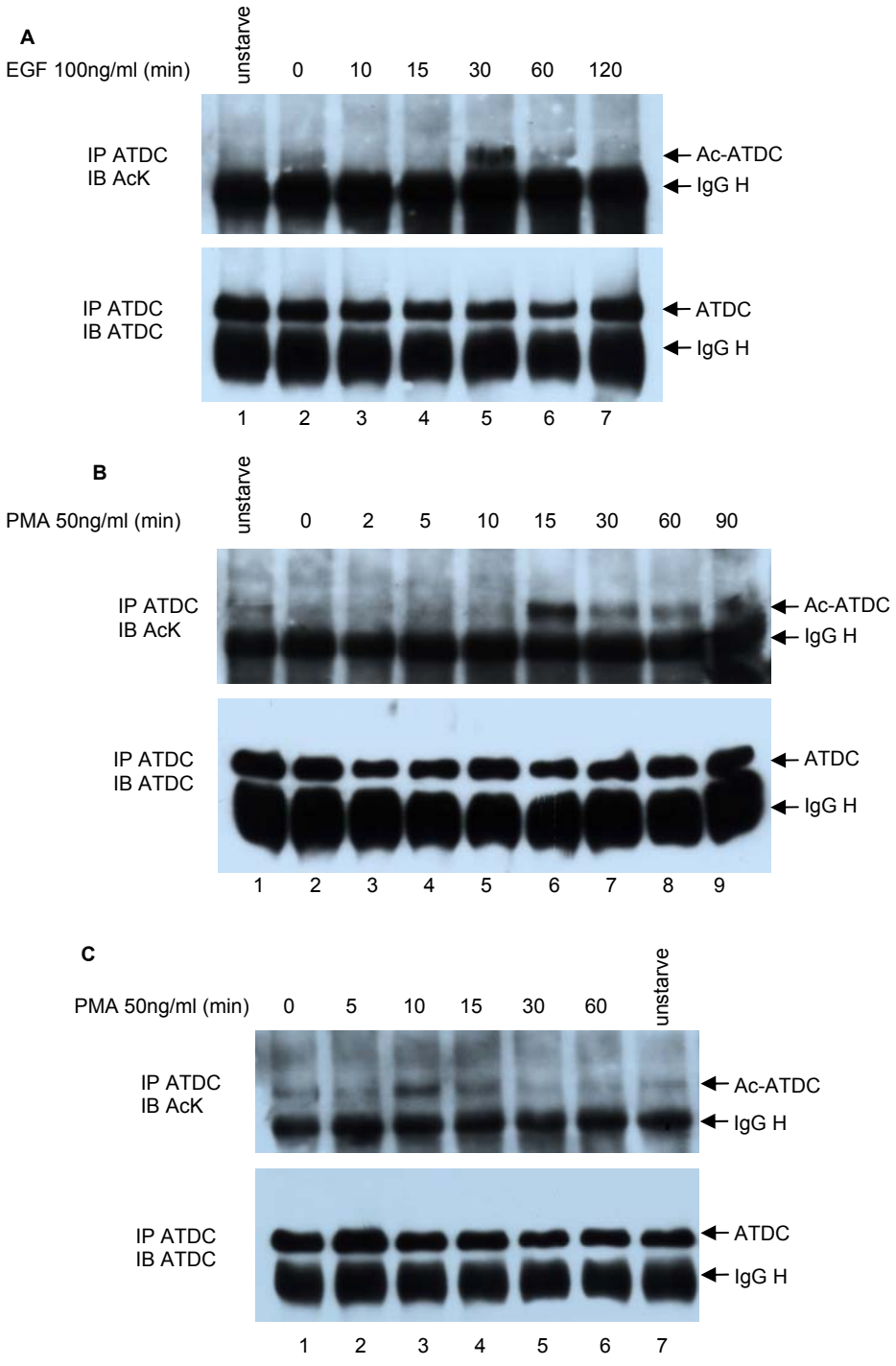
A
EGF 100ng/ml (min)
unstarve
0
10
15
30
60
120
IP ATDC
IB AcK
Ac-ATDC
IgG H
IP ATDC
IB ATDC
ATDC
IgG H
1
2
3
4
5
6
7
B
PMA 50ng/ml (min)
unstarve
0
2
5
10
15
30
60
90
IP ATDC
IB AcK
Ac-ATDC
IgG H
IP ATDC
IB ATDC
ATDC
IgG H
1
2
3
4
5
6
7
8
9
C
PMA 50ng/ml (min)
0
5
10
15
30
60
unstarve
IP ATDC
IB AcK
Ac-ATDC
IgG H
IP ATDC
IB ATDC
ATDC
IgG H
1
2
3
4
5
6
7

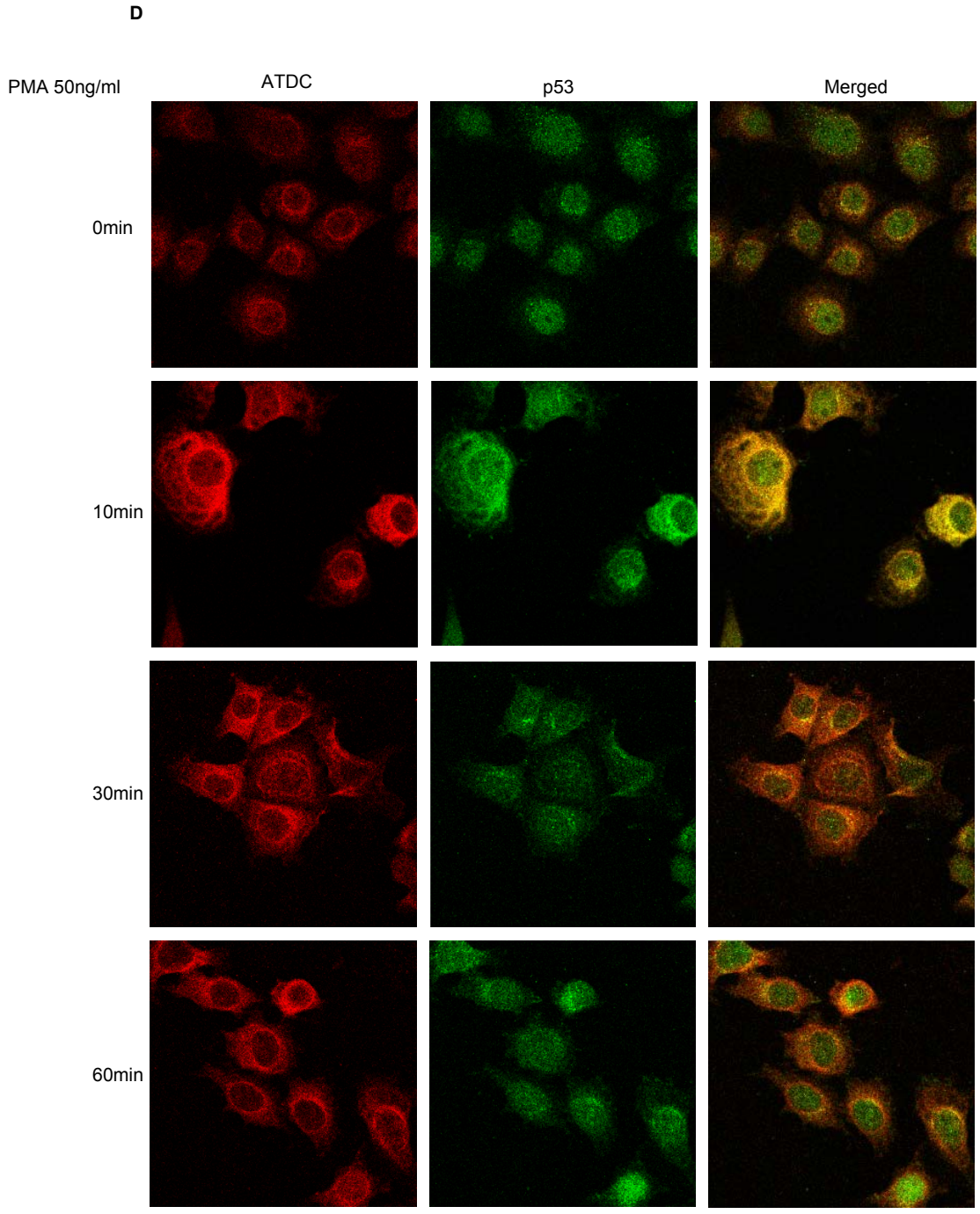

Figure 18. Growth stress regulates ATDC acetylation

(A) HeLa cells were starved for 18hr, and treated with EGF (100ng/ml) or left untreated as indicated. Cell lysates were then immunoprecipitated under high stringency conditions with anti-ATDC antibodies. Endogenous acetylated ATDC was analyzed by Western blotting with a mixture of polyclonal anti-acetyl-lysine antibodies. (B) HeLa cells were starved for

18hr, and treated with PMA (50ng/ml) or left untreated as indicated. Acetylation of endogenous ATDC was analyzed as in Panel A. (C) SiHa cells were starved for 18hr, and treated with PMA (50ng/ml) or left untreated as indicated. Acetylation of endogenous ATDC was analyzed as in Panel A. (D) SiHa cells were starved for 18hr, and treated with PMA (50ng/ml) or left untreated as indicated. Cells were fixed, permeabilized, and stained with anti-ATDC and anti-p53 DO-1 antibodies, followed by Alexa-555 and Alexa-488-conjugated secondary antibodies, and analyzed using Zeiss Confocal Microscopy.

Interestingly, we found that ATDC interacts with p53 in SiHa cell cytoplasm in a growth stress-inducible manner (Figure 18D), which could be correlated with growth stress-induced ATDC acetylation (Figure 18C). These data suggested that ATDC acetylation, which could be regulated by growth factors in tumor microenvironment, might be helpful for tumor cells to resist ionizing radiation therapy and survive.

Dissussion

The present data reveal that ATDC, the product of the ataxia-telangiectasia group D complementing gene, is acetylated dynamically within the cells in a growth stress stimulation manner. And HDAC9 and p300 acetyltransferase as its interaction partners play important roles to balance ATDC reversible acetylation. Importantly, ATDC is a cytoplasmic protein that is critically involved in the regulation of p53 subcellular localization and subsequent function in cells. HDACs play critical roles in diverse biological functions (Ruijter et al., 2003; Marks et al., 2003). The HDAC9 mutant mice displays an enhanced response to stress signals and enhanced hypertrophic phenotype (Zhang et al., 2002), suggesting this HDAC acts in the adult heart to suppress the fetal gene program and hypertrophic growth. And this function was carried out by forming a complex

with an important transcription factor MEF2 (the myocyte enhancer-binding factor 2) (Zhang et al., 2002; Haberland et al., 2007). In this study, using immunoaffinity purification method, we identify another important HDAC9 interaction partner ATDC. Through preventing the ATDC-p53 complex formation, HDAC9 could sensitize the tumor cells with a radio-resistant phenotype caused by abnormal expression of ATDC. These data would have an important implication for future clinical radio-therapy for cancer.

The molecular basis of the defect in AT is still largely unknown, although the diversity of phenotypes has led to the suggestion that a signaling mechanism may be defective. ATDC, which complements the ionizing radiation sensitivity of AT group D cell lines, might involve in a signal transduction pathway that is induced by ionizing radiation. It has been previously reported that it could physically interact with vimentin, a type III intermediate filament; with hPKCI-1, a small protein inhibitor of PKC (Brzoska et al., 1995). Some experiments data suggested aberrant p53 function may be a major factor in the hypersensitivity of AT cells to ionizing radiation (Meyn et al., 1994). In the current study, ATDC was found it could physically interact and colocalize with p53 in the cell cytoplasm. By controlling p53 subcellular localization and its subsequent biological function, ATDC could facilitate the cell survival under γ-irradiation stress. Taken together, these data suggest a model in which ATDC-p53 complex involves in an ionizing radiation-induced signal transduction pathway.

As a transcription factor, nuclear localization of p53 is essential for its role in tumor suppression (Vousden et al., 2002; Jimenez et al., 1999). However, p53 is diffusely distributed in the cytoplasm of normal unstressed cells; many types of tumors cells have abnormal cytoplasmic localization of p53 and an impaired p53-dependent stress response despite the fact that they express wild-type p53 proteins (Jimenez et al., 1999; Moll et al., 1996). In previous studies, it has been shown that the majority of cytoplasmic p53 is tightly associated with endogenous Parc (p53-associated, Parkin-like cytoplasmic protein) (Nikolaev et al., 2003). In the absence of stress, inactivation of endogenous Parc leads p53 activation through inducing p53 nuclear localization. In current study, ATDC was also found has a similar role as Parc in regulating p53 function. Furthermore, ATDC-p53 complex formation is regulated by ATDC K116 acetylation, which is controlled by HDAC9. And our results also indicate that the levels of ATDC proteins are relatively high in cervical and pancreatic carcinoma cell lines and pancreatic tumor tissues. It is conceivable, therefore, that the high levels of ATDC in these cells may prevent nuclear translocation of p53, even in the presence of genotoxic stress although other mechanisms may also contribute to this phenomenon. In consistence with this notion, we have also shown that shRNA-mediated reduction of ATDC protein levels or introduction of HDAC9 can restore a strong p53-dependent stress response in cervical carcinoma SiHa cells. As such, the ATDC-mediated pathway of p53 regulation may prove to be a potential target for cancer therapy. In particular, agents that down-regulate ATDC protein levels or abrogate

the ATDC-p53 interaction, such as introduction of HDAC9, may sensitize tumor cells to p53-dependent apoptosis.

As an acetylated protein, p53 function was directly regulated by a class I HDAC, HDAC1 (Luo et al., 2000), and a class III HDAC, SIRT1 (Luo et al., 2001; Vaziri et al., 2001). In current study, we report a class II HDAC, HDAC9 could indirectly regulate p53-mediated apoptotic pathway by regulating its interaction with ATDC. These data suggest HDACs play much wider roles in cells in addition to their transcriptional repression function.

References

1. Aizawa, H., Hu, S.C., Bobb, K., Balakrishnan, K., Ince, G., Gurevich, I., Cowan, M., and Ghosh, A. (2004). Dendrite development regulated by CREST, a calcium-regulated transcriptional activator. Science 303, 197-202.
2. Brzoska, P.M., Chen, H., Zhu, Y., Levin, N.A., Disatnik, M.H., Mochly-Rosen, D., Murnane, J.P., Christman, M.F. (1995). The product of the ataxia-telangiectasia group D complementing gene, ATDC, interacts with a protein kinase C substrate and inhibitor. Proc Natl Acad Sci U S A. 92(17):7824-8.
3. Chan, H.M., Krstic-Demonacos, M., Smith, L., Demonacos, C., La Thangue, N.B. (2001). Acetylation control of the retinoblastoma tumour-suppressor protein. Nat Cell Biol. 3(7):667-74.
4. Chong, M. J., Murray, M.R., Gosink, E.C., Russell, H.R., Srinivasan, A., Kapsetaki, Korsmeyer, S.J., McKinnon, P.J. (2000). Atm and Bax cooperate

in ionizing radiation-induced apoptosis in the central nervous system. Proc. Natl Acad. Sci. USA 97, 889-894.

5. Glozak, M.A., Sengupta, N., Zhang, X., and Seto, E. (2005). Acetylation and deacetylation of non-histone proteins. Gene 363, 15-23.
6. Gray, S.G., and Ekstrom, T.J. (2001). The human histone deacetylase family. Exp. Cell Res. 262, 75-83.
7. Gregoretti, I.V., Lee, Y.M., and Goodson, H.V. (2004). Molecular evolution of the histone deacetylase family: functional implications of phylogenetic analysis. J. Mol. Biol. 338, 17-31.
8. Haberland, M., Arnold, M.A., McAnally, J., Phan, D., Kim, Y., Olson, E.N. (2007). Regulation of HDAC9 gene expression by MEF2 establishes a negative-feedback loop in the transcriptional circuitry of muscle differentiation. Mol Cell Biol. 27(2):518-25.
9. Hassig, C.A., and Schreiber, S.L. (1997). Nuclear histone acetylases and deacetylases and transcriptional regulation: HATs off to HDACs. Curr. Opin. Chem. Biol. 1, 300-308.
10. He, T.C., Zhou, S., da Costa, L.T., Yu, J., Kinzler, K.W., Vogelstein, B. (1998). A simplified system for generating recombinant adenoviruses. Proc Natl Acad Sci U S A. 95(5):2509-14.
11. Herzog, K. H., Chong, M. J., Kapsetaki, M., Morgan, J. I., McKinnon, P. J. (1998). Requirement for Atm in ionizing radiation-induced cell death in the developing central nervous system. Science 280, 1089-1091.

12. Hosoi, Y., Kapp, L.N. (1994). Expression of a candidate ataxia-telangiectasia group D gene in cultured fibroblast cell lines and human tissues. Int J Radiat Biol. 66(6 Suppl):S71-6.
13. Iacobuzio-Donahue, C.A., Maitra, A., Shen-Ong, G.L., van Heek, T., Ashfaq, R., Meyer, R., Walter, K., Berg, K., Hollingsworth, M.A., Cameron, J.L., Yeo, C.J., Kern, S.E., Goggins, M., Hruban, R.H. (2002). Discovery of novel tumor markers of pancreatic cancer using global gene expression technology. Am J Pathol. 160(4):1239-49.
14. Jimenez, G.S., Khan, S.H., Stommel, J.M. and Wahl, G.M. (1999). p53 regulation by post-translational modification and nuclear retention in response to diverse stresses. Oncogene 18, pp. 7656–7665.
15. Johnson, C.A., and Turner, B.M. (1999). Histone deacetylases: complex transducers of nuclear signals. Semin. Cell Dev. Biol. 10, 179-188.
16. Johnstone, R.W., Licht, J.D. (2003). Histone deacetylase inhibitors in cancer therapy: is transcription the primary target? Cancer Cell. 4(1):13-8.
17. Jung, M., Zhang, Y., Dimtchev, A., and Dritschilo, A. (1998). Impaired regulation of nuclear factor-kappaB results in apoptosis induced by gamma radiation. Radiat. Res. 149, 596–601.
18. Kouzarides, T. (2000). Acetylation: a regulatory modification to rival phosphorylation? EMBO J. 19, 1176-1179.
19. Kramer, O.H., Gottlicher, M., Heinzel, T. (2001). Histone deacetylase as a therapeutic target. Trends Endocrinol Metab. 12(7):294-300.

20. Kuo, M.H., and Allis, C.D. (1998). Roles of histone acetyltransferases and deacetylases in gene regulation. Bioessays 20, 615-626.

21. Kapp, L.N., Painter, R.B., Yu, L.C., van Loon, N., Richard, C.W. 3rd, James, M.R., Cox,. D.R., Murnane, J.P. (1992). Cloning of a candidate gene for ataxia-telangiectasia group D. Am J Hum Genet. 51(1):45-54.

22. Laderoute, K.R., Knapp, A.M., Green, C.J., Sutherland, R.M., Kapp, L.N. (1996). Expression of the ATDC (ataxia telangiectasia group D-complementing) gene in A431 human squamous carcinoma cells. Int J Cancer. 66(6):772-8.

23. Lee, Y., Chong, M. J., McKinnon, P. J. (2001). Ataxia telangiectasia mutated-dependent apoptosis after genotoxic stress in the developing nervous system is determined by cellular differentiation status. J. Neurosci. 21, 6687-6693.

24. Leonhardt, E.A., Kapp, L.N., Young, B.R., Murnane, J.P. (1994). Nucleotide sequence analysis of a candidate gene for ataxia-telangiectasia group D (ATDC). Genomics. 19(1):130-6.

25. Luo, J., Su, F., Chen, D., Shiloh, A., Gu, W. (2000). Deacetylation of p53 modulates its effect on cell growth and apoptosis. Nature. 408(6810):377-81.

26. Luo, J., Nikolaev, A.Y., Imai, S., Chen, D., Su, F., Shiloh, A., Guarente, L., and Gu, W. (2001). Negative control of p53 by Sir2alpha promotes cell survival under stress. Cell 107, 137-148.

27. Mahlknecht, U., Schnittger, S., Will, J., Cicek, N., Hoelzer, D. (2002). Chromosomal organization and localization of the human histone deacetylase 9 gene (HDAC9). Biochem Biophys Res Commun. 26;293(1):182-91.

28. Marks, P.A., Miller, T., and Richon, V.M. (2003). Histone deacetylases. Curr. Opin. Pharmacol. 3, 344-351.

29. Meyn, M.S., Strasfeld, L., Allen, C. (1994). Testing the role of p53 in the expression of genetic instability and apoptosis in ataxia-telangiectasia. Int J Radiat Biol. 66(6 Suppl):S141-9.

30. Moll, U.M., Ostermeyer, A.G., Haladay, R., Winkfield, B., Frazier, M. and Zambetti, G. (1996). Cytoplasmic sequestration of wild-type p53 protein impairs the G1 checkpoint after DNA damage. Mol. Cell. Biol. 16, pp. 1126–1137.

31. Nikolaev, A.Y., Li, M., Puskas, N., Qin, J., G,u W. (2003). Parc: a cytoplasmic anchor for p53. Cell. 112(1):29-40.

32. Peng, Y., Li, C., Chen, L., Sebti, S., Chen, J. (2003). Rescue of mutant p53 transcription function by ellipticine. Oncogene. 22(29):4478-87.

33. Petrie, K., Guidez, F., Howell, L., Healy, L., Waxman, S., Greaves, M., Zelent, A. (2003). The histone deacetylase 9 gene encodes multiple protein isoforms. J Biol Chem. 278(18):16059-72.

34. Peterson, C.L. (2002). HDAC's at work: everyone doing their part. Mol. Cell 9, 921-922.

35. Reymond, A., Meroni. G., Fantozzi, A., Merla, G., Cairo, S., Luzi, L., Riganelli, D., Zanaria, E., Messali, S., Cainarca, S., Guffanti, A., Minucci, S., Pelicci, P.G,, Ballabio, A. (2001). The tripartite motif family identifies cell compartments. EMBO J. 20(9):2140-51.

36. Rezai-Zadeh, N., Tsai, S.C., Wen, Y.D., Yao, Y.L., Yang, W.M., Seto, E. (2004). Histone deacetylases: purification of the enzymes, substrates, and assay conditions. Methods Enzymol. 377:167-79.

37. Ruijter, A.J.M., van Gennip, A.H., Caron, H.N., Kemp, S., and van Kuilenburg, A.B.P. (2003). Histone deacetylases (HDACs): characterization of the classical HDAC family. 370, 737-749.

38. Sawada, M., Sun, W., Hayes, P., Leskov, K., Boothman, D.A., Matsuyama, S. (2003). Ku70 suppresses the apoptotic translocation of Bax to mitochondria. Nat Cell Biol. 5(4):320-9.

39. Vaziri, H., Dessain, S.K., Ng Eaton, E., Imai, S.I., Frye, R.A., Pandita, T.K., Guarente, L., and Weinberg, R. A. (2001). hSIR2(SIRT1) functions as an NAD-dependent p53 deacetylase. Cell 107, 149-159.

40. Vousden, K.H. (2002). Activation of the p53 tumor suppressor protein. Biochim. Biophys. Acta 1602, pp. 47–59.

41. Yang, X.J., Ogryzko, V.V., Nishikawa, J., Howard, B.H., and Nakatani, Y. (1996). A p300/CBP-associated factor that competes with the adenoviral oncoprotein E1A. Nature 382, 319-324.

42. Yang, X.J., and Seto, E. (2003). Collaborative spirit of histone deacetylases in regulating chromatin structure and gene expression. Curr. Opin. Genet. Dev. 13, 143-153.

43. Yang, X.J. (2004). Lysine acetylation and the bromodomain: a new partnership for signaling. Bioessays 26, 1076-1087.

44. Zhang, C.L., McKinsey, T.A., Chang, S., Antos, C.L., Hill, J.A., Olson, E.N. (2002). Class II histone deacetylases act as signal-responsive repressors of cardiac hypertrophy. Cell. 110(4):479-88.

45. Zhang, Q., Yao, H., Vo, N., and Goodman, R.H. (2000). Acetylation of adenovirus E1A regulates binding of the transcriptional corepressor CtBP. Proc. Natl. Acad. Sci. USA 97, 14323-14328.

46. Zhang, X., Wharton, W., Yuan, Z., Tsai, S.C., Olashaw, N., Seto, E. (2004). Activation of the growth-differentiation factor 11 gene by the histone deacetylase (HDAC) inhibitor trichostatin A and repression by HDAC3. Mol Cell Biol. 24(12):5106-18.

47. Zhang, Y., Dimtchev, A., Dritschilo, A., and Jung, M. (2001). Ionizing Radiation-induced Apoptosis in Ataxia-Telangiectasia Fibroblasts. JBC. 276(31):28842–28848.

48. Zhang, Z., Gerhard, D.S., Nguyen, L., Li, J., Traugott, A., Huettner, P.C., Rader, J.S. (2005). Fine mapping and evaluation of candidate genes for cervical cancer on 11q23. Genes Chromosomes Cancer. 43(1):95-103.

49. Zhao, S., Renthal, W., and Lee, E.Y. (2002). Functional analysis of FHA and BRCT domains of NBS1 in chromatin association and DNA damage responses. Nucleic Acids Res. 30, 4815-4822.

50. Zhou, X., Marks, P.A., Rifkind, R.A., Richon, V.M. (2001). Cloning and characterization of a histone deacetylase, HDAC9. Proc Natl Acad Sci U S A. 98(19):10572-7.

ABOUT THE AUTHOR

Zhigang Yuan was born in Shanxi, China in a family of 3 children. After 5 years study at the medical college of Jilin university (the former Norman Bethune university of medical sciences), Changchun, China, Mr. Yuan received his bachelor degree of medicine in the summer of 1999. He went on pursuing his master degree in the department of immunology at the medical center of Fudan university (the former Shanghai medical university), Shanghai, China from August, 1999 to June, 2002. In August, 2002, Mr. Yuan was enrolled in the Ph.D. program in the department of molecular medicine at the University of South Florida's college of medicine, Tampa, Florida. While enrolling in the Ph.D. program, the American Heart Association granted Mr. Yuan a two-year predoctoral fellowship for his innovative research proposal.